UNIVERSITY OF OSLO
Department of Geosciences

A study of transport and deposition of black carbon using the Oslo CTM2 chemical transport model; A comparison of two aerosol parameterizations

Master thesis in Geosciences

Marianne Tronstad Lund

02.06.2008

Acknowledgements

First and foremost, I want to thank my guidence counselor, Terje K. Berntsen at CICERO, for help and feedback throughout this work. And a big thank you to Amund Søvde for all his help with the model, and for answering my numerous questions about IDL programming. I would also like to thank Alf Grini, Tore F. Berglen and Ole Kristian Kvissel for helping me get started with the model and programming. And Ragnhild B. Skeie for the use of her fortran programmes. I also have to thank Gunnar Wollan and Kjell Andresen for fixing all computer problems, and my father and my boyfriend for their feedback.

Finally, a thank you to fellow students for useful discussions and answers.

Abstract

The chemical transport model Oslo CTM2 has been used to test two different parameterizations of the black carbon (BC) aerosol. Key uncertainties associated with the representation aerosols in modeling are size distribution, mixing state and removal processes. An important parameter for black carbon is the aging time. In the original aerosol parameterization, aging was represented by a constant transfer of 24% per day from hydrophobic to hydrophilic mode. A new aerosol parameterization called M7, which gives a more physical representation of BC aging by including particle interaction, was recently included in the CTM2 model. This module describes size distribution, mixing state and particle interaction for sulphur, dust, black and organic carbon and sea salt.

In this thesis, several simulations have been done to test the effect of using M7 on the modeled BC distribution, lifetime, deposition and regional contributions. Applying the M7 module results in regional and seasonal differences in BC aging. In high-latitudes, the aging is slower than with the original version, leading to an increased burden of mainly insoluble BC particles. Between $30\,^{\circ}N$ and $30\,^{\circ}S$ the burden is reduced, indicating a shorter lifetime caused by faster aging. Global mean BC lifetime and burden is only slightly changed; from 7.63 days and 0.17 Tg with the original parameterization to 7.3 days and 0.14 Tg.

Modeled BC content in Arctic snow and ice show high concentrations on the continents, and maximum near industrialized areas. Concentrations in the snow and ice in the Arctic Ocean are mostly less than 10 $ng\ g^{-1}$ with both aerosol representations.

Regional experiments with emissions in China and Europe separately, show that European emissions contribute most to total BC burden north of $60\,^{\circ}N$ in the lower atmosphere, while emissions from China are important above $6\,km$. European emissions also provide the largest contribution to accumulated BC in snow and ice north of $60\,^{\circ}N$. These results are consistent with

several other studies. The choice of aerosol parameterization strongly influences the regional impact. BC aging time in China is reduced from 4.16 days in the original version to 3.16 days with M7, while aging time in Europe is increased to 5.16 days. As a consenquence, the contribution from China to atmospheric BC burden and to accumulated BC in snow and ice is reduced, while the European contributions are strenghtened.

There is potential for improvement in the M7 module. However, the regional and seasonal variation in BC aging is captured, and there does not appear to be any large errors in the model results compared to previous calculations and observations. M7 allow for a closer study of regional impact and interaction between co-emitted pollutants, and may improve the calculation of radiative forcing.

Contents

Chapter 1

Introduction

The focus on global climate change has increased dramatically in the recent years. In 2007, the fourth report from the Intergovernmental Panel on Climate Change (IPCC) was published. It concludes with a high degree of scientific certainty that anthropogenic activity has contributed to the observed global warming (IPCC, 2007). The most important components in the climate discussion are the long-lived greenhouse gases, and especially CO_2. However, climate change is a complex problem involving many atmospheric components, processes and feedbacks. It may be necessary to consider other atmospheric constituents, including aerosols, when discussing cost-effective mitigation options.

Atmospheric aerosol is the suspension of liquid or solid particles in the air and it plays an important role in the global climate system. Anthropogenic activity has strongly increased the global aerosol burden from preindustrial times. Aerosol particles affect the climate system via several physical mechanisms. Aerosols can be scattering or absorbing, both in the shortwave and the longwave range. They can also affect the amount and coverage of clouds and the precipitation efficiency by acting as cloud condensation nuclei and ice nuclei. Furthermore, they can affect the hydrological cycle, the surface energy budget and the surface albedo (Lohmann and Feichter, 2005). This thesis focuses on the black carbon aerosol [1]. BC is the optically absorbing part of the soot and smoke produced during incomplete combustion. The absorbing property means BC has a potentially strong warming effect, but in contrast to CO_2, which remains in the atmosphere more than 100 years, BC has an atmospheric lifetime of days.

[1] henceforth abbreviated BC

Reducing BC could contribute to a slowing down of the global warming, and the effects of reduction efforts would become evident much sooner than for the long-lived gases. Because of this, many believe that BC should be included in global climate mitigation strategies (Bond (2007), Jacobson (2002), Hansen et al. (2000)).

Today, climate policies are based on the assumption that the location of emission has no effect on the climate impact of the gas (Rypdal et al., 2005). This may not be the case for short-lived species such as aerosols. Several studies have found regional and sectoral differences in burden and radiative forcing (Berntsen et al. (2006), Koch et al. (2007)). The composition of emissions and the regional meteorological, dynamical and chemical conditions affect aging and lifetime. For example, emissions of BC from biomass burning are much higher in Africa than in South America, but South America has a larger contribution to BC burden (Koch et al., 2007). This is because African emissions are more heavily weighted towards the Equator and are more efficiently scavenged. Radiative forcing also depends on the physical properties of the earth-atmosphere system, such as clouds, relative humidity and temperature profile (Rypdal et al., 2005). In addition there are economic and political considerations. Mitigations can therefore be more effective in some source regions than others, and it is important to investigate regional impact.

The following section describes the objective of this thesis, and also the purpose and background for the experiments conducted. The chemical transport model Oslo CTM2 is used to study the transport, distribution and deposition of BC particles. Key uncertainties in the treatment of aerosols are the size distribution and composition of particles. In the atmosphere, each aerosol particle in a population can consist of both scattering and absorbing material, i.e. it is internally mixed. Such mixtures are formed because particles interact with each other as they become soluble and grow. Many models, including the Oslo CTM2, have until now only treated the total mass of aerosols species and considered each species as separate from the others. New parameterizations allow a more physically correct representation. Such a parameterization, called M7 (Vignati and Wilson, 2004), was recently implemented in the Oslo CTM2 model. The M7 module has separate, internally mixed modes for particles with radius within defined intervals, and particles are moved to the next mode as they grow. Sulphuric acid, BC, OC, dust and sea salt are included in the module. Most BC is emitted as hydrophobic, i.e. insoluble, particles. Previously the model represented the aerosol aging by pre-determined, constant transfer rates from insoluble to soluble mode. In M7, particles

become hydrophilic through coating by sulphuric acid and by coagulation with other soluble aerosols. This leads to regional and seasonal differences aging time depending on the availability of these species. The processes of coagulation and condensation also leads to particle growth. M7 thus gives a dynamical description of the evolution of the size distribution of aerosols (Vignati and Wilson, 2004). M7 also includes the important interaction between different aerosol species, giving an internally mixed aerosol population. This is important because both size and mixing state have important implications for aerosol optical properties and removal processes.

The objective in this thesis is to study how M7 affects the model representation of BC aerosols. Originally, the transfer rate used in the CTM2 model was almost 60% per day, taken from a study by Cooke et al. (1999), but the resulting concentration was underestimated compared to observations. To get a better match, the lifetime of BC was increased by reducing the transfer rate to 24% per day (Maria et al., 2004). The modeled concentrations with the original aerosol parameterization should therefore be in good agreement with other studies and observations already. Here, the hypothesis that using more realistic parameterization of BC aging as in M7 should improve the model performance is investigated. The first part of the results include a general description of BC burden, lifetime, and distribution, first with the original aerosol representation and then with M7. In addition, several simulations are conducted to test the importance of the wet removal mechanisms for BC.

The concentration of BC in snow and ice, and the effect of using M7, is also studied. In the version of the CTM2 model used here, a routine which models deposition and accumulation of BC in snow and ice is included (Skeie, 2007). Pure, new snow has an albedo of $0.8 - 0.95$ and acts to cool the climate system by reflecting almost all incoming solar radiation. When deposited in snow and ice BC reduces the surface albedo and increases absorption. This triggers strong postitive climate feedbacks and result in a warming effect. It is therefore important to be able to model the content of BC in snow and ice, and an important part of the work in this thesis is to extend the routine so it can be combined with M7.

To investigate regional and seasonal contributions to distribution, burden and deposition, and the regional variation in BC aging with M7, the model is run with emissions from separate geographical areas with both aerosol parameterizations. The focus is on mid- and high northern latitudes. When constant transfer to hydrophilic mode is used, the aging time is the same for particles in all parts of the world. With M7, the regional and

seasonal differences in BC aging from particle interaction should become evident. Large emissions of SO_2 and effective production of sulphuric acid should lead to a more rapid aging. The BC lifetime may thus be reduced compared to the original version as particles can be removed earlier. A higher aging time is expected for BC in regions with less sulphuric acid. Europe and China are chosen as the two regions to study, both because they have different conditions in terms of convection and precipitation, and because of the different emission trends. In Europe, emissions of SO_2 have decreased by $60 - 80\%$ in the past few decades (Vestreng et al., 2007), while in China BC and SO_2 emissions are large and increasing (Novakov et al., 2003).

Since BC deposited in snow and ice has important climate effects, the focus is on regional contributions to BC in the Arctic. The Arctic troposphere, the region north of $70\,^{\circ}N$, is isolated from the rest of the atmosphere by a transport barrier called the Arctic front. To be able to cross this barrier, airmasses must have low potential temperature. Otherwise they are forced to ascend and do not reach lower altitudes in the Arctic. To what extent different source regions contribute to the BC in the Arctic troposphere is uncertain, and especially the magnitude of Chinas contribution is debated. Koch and Hansen (2005) suggest that the dominating source of Arctic BC is South Asia. However, this result has been questioned (Stohl (2006)), because direct transport from southeast Asia to the Arctic troposphere is not possible due to the large temperature difference (Law and Stohl, 2007). Stohl (2006) investigated the role of transport into the Arctic troposphere and found that most BC in the Arctic troposphere originates from sources in Europe and Eurasia. Neither of these articles considered the BC concentration in snow, but in this thesis both regional contributions to BC in the Arctic atmosphere and to concentration in snow and ice in the Arctic is studied. The changes in aging when the M7 module is used are expected to affect BC deposition. One important question is which region originally contributes most to the BC in Arctic snow and ice and how M7 changes this.

Finally, an experiment to further investigate the BC/ sulphuric acid interaction in M7 is conducted. Emission of SO_2 in Europe is increased by 70% to imitate previous levels, and the resulting effect on burden, zonal distribution and deposition is studied. Since a faster aging and following wet removal closer to the source is expected, the hypothesis is that the concentration of BC in snow and ice in the Arctic is reduced.

Several other studies of BC have been done. Near-surface concentration

from the work done here is compared with results modeled by Jacobson (2002) and with observations summarized in the same article, and with results from Koch et al. (2007). Regional contributions are also compared with those in Koch et al. (2007). The BC concentration in snow and ice is compared with modeled results from Flanner et al. (2007) and with available observations.

Chapter 2 contains theory, and Chapter 3 describes the CMT2 model and experiments. In Chapter 4 the results are presented and discussed, followed by the conclusion in Chapter 5. There are of course many more useful tests and simulations which there is simply not enough time for in a master's degree, and a brief outlook for further work with the subjects covered here completes this thesis.

Chapter 2

Theory

2.1 Black carbon emissions

BC is produced during incomplete combustion of fossil fuel (oil and gas) and biofuel (charcoal and dung), and from biomass burning (grass and forest fires). Total global BC emissions are estimated around $7.7 Tg/yr$ with an uncertainty factor of two (Bond et al., 2006). Approximately 40% is from the use of fossil fuel, 20% from biofuel and 40% from biomass burning. The main source regions are industrialized areas in the Northern Hemisphere, as well as regions with biomass burning in South America and Central Africa. There are also areas of forest fires in the Northern Hemisphere, mainly Canada and Siberia, during the summer.

Figure 2.1 shows the global distribution of BC emissions, and Figure 2.2 shows the contribution from various sectors in different the regions to the total emission. In Africa and Latin America the major sectors are burning of savanna and forest, while the largest emissions in India and China are from the use of coal and biofuels. In Europe, North America and former USSR there is a more equal partitioning between sectors, with the use of coal and diesel being slightly larger than the other sectors. During the last 50 years there has been a change in the regional emission pattern of fossil fuel BC (Novakov et al., 2003). In Europe, the former USSR and USA emissions have decreased significantly. This is due to measures targeted at reducing emissions, such as filters in diesel engines, improved combustion technology and a strong decrease in the use of coal, specially in Eastern Europe. China and India have experienced strong developement and

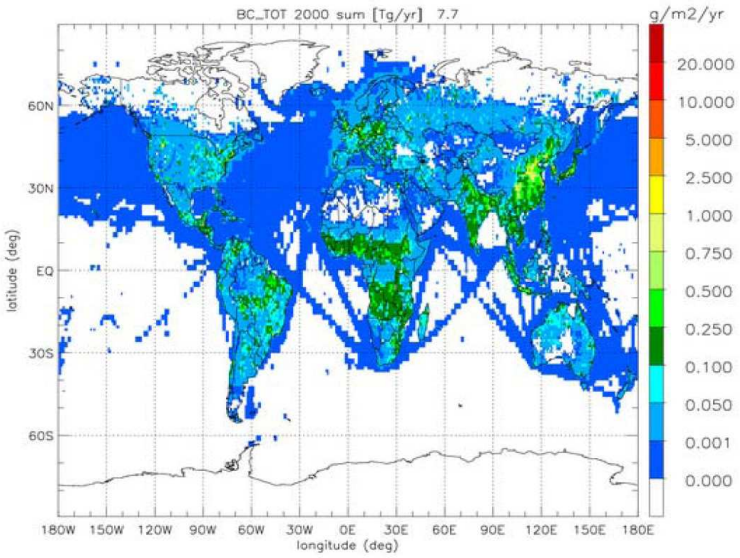

Figure 2.1: *Global distribution of BC emissions in $g/m^2/yr$ from Bond et al. (2006)*

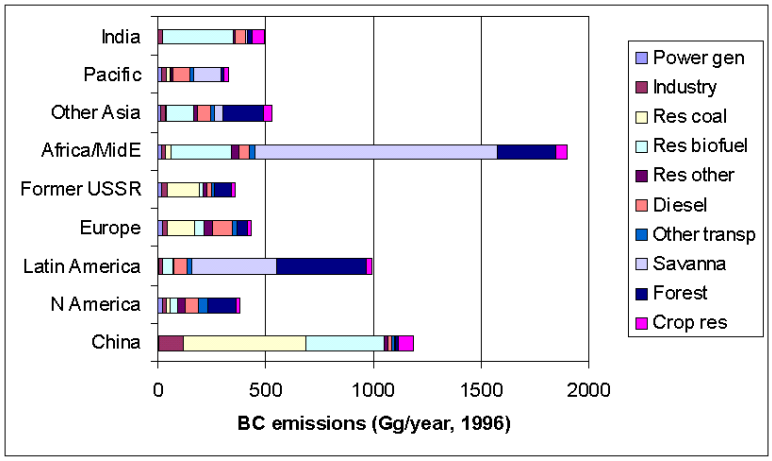

Figure 2.2: *Contributions from different sectors in different regions to total BC emissions in the area in Gg/yr, (Bond et al.)*

economic growth, and now are the largest contributors to fossil fuel BC. One set of new estimates indicate that BC emissions in China have almost doubled from 2000 to 2006, and that SO_2 emissions have increased by 50% (http://www.cgrer.uiowa.edu/EMISSION_DATA_new/summary_of_ changes.html).

2.2 Effects on climate

The climate impact of BC is a result of many complex processes. BC can reduce planetary albedo through several mechanisms (Ramanathan and Carmichael, 2008). First of all, BC particles absorb both direct and reflected solar radiation, leading to a significant warming of the atmosphere. BC has opposing effects in the atmosphere and at the surface (Ramanathan and Carmichael, 2008). Absorption in higher atmospheric levels reduces the amount of solar radiation reaching the surface, leading to a negative radiative forcing there, so-called surface dimming. The resulting top of the atmosphere (TOA) direct forcing of BC is, however, positive, and estimates of the magnitude range from $+0.2\ Wm^{-2}$ in the latest IPCC report to $+0.9\ Wm^{-2}$ in Ramanathan and Carmichael (2008). These estimates do not include the effect on snow albedo or on clouds as there are large uncertainties related to these. In contrast, estimated radiative forcing from tropospheric ozone and methane is $+0.35\ Wm^{-2}$ and $+0.48\ Wm^{-2}$ (IPCC, 2007), so BC is a strong warming component.

The second way BC reduces planetary albedo is through its effects on cloud cover and cloud albedo. Traditionally, increased aerosol concentration is expected to result in more, but smaller cloud droplets. This increases reflection of solar radiation directly by increasing total area, and indirectly by increasing cloud lifetime and coverage due to reduced precipitation efficiency (Lohmann and Feichter, 2005). These two effects are called the cloud albedo and cloud lifetime effect, and the resulting forcing is negative. Several studies have indicated that absorbing aerosols, however, can strongly reduce low-level cloud cover by heating the air and evaporating cloud droplets (Johnson et al. (2004), Ackerman et al. (2000), Koren et al. (2004)). Increased aerosol consentrations can also reduce cloud cover through surface dimming. Less energy reaching the surface results in a more stable and dry atmosphere, which inhibits new cloud formation (Koren et al., 2004). This has been named the semi-direct effect. The studies mentioned above give very different results for the magnitude of this effect, and even the sign of the forcing is uncertain. A larger fraction

of absorbing material in cloud drops also reduce cloud albedo directly. Lohmann and Diehl (2005) suggested that if a fraction of the hydrophilic BC acts as a contact ice nuclei, an increase in the concentration could lead to more rapid glaciation, i.e. complete freezing of the cloud, and increased precipitation via the ice phase. Again, the result is reduced cloud cover and decreased planetary albedo, which leads to more absorption of solar radiation within the earth-atmosphere system and a further warming.

Finally, BC plays an important role both before and after deposition in snow and ice covered areas. The direct effect of BC is much stronger over surfaces with high albedo due to the high contrast and multiple scattering between the surface and aerosol layer. At the same time, the cooling aerosols emitted together with BC (organic carbon, sulphur) have little effect over bright surfaces due to low contrast. Last, but not least, BC exerts a warming effect after it is deposited on the surface. Flanner et al. (2007) found that even small quantities of black carbon reduce snow reflectance. Using their snow, ice, and aerosol radiative model, coupled with a general circulation model, they estimated a global mean BC/snow surface radiative forcing of $+0.054\ Wm^{-2}$. Their results also suggested that nearly 80% of this forcing is due to anthropogenic activity. Hansen and Nazarenko (2004) estimated a forcing of $+0.3\ Wm^{-2}$ in the Northern Hemisphere and the best estimate from IPCC (2007) is $+0.1\ Wm^{-2}$.

Although the forcing is not too large, the reduction of snow/ice albedo is a concern due to the strong positive feedbacks involved. Flanner et al. (2007) mentions several of these. Absorption can change the snowmelt onset and speed, and thus the spatial coverage of snow/ice. This reveals the darker underlying surface which absorbs much more solar radiation, leading to further reduction in snow cover. When the temperature of the snow increases, the snow becomes more coarse grained. This darkens the snow directly, but it also increases the absorption for a certain amount of BC. This is because solar radiation can penetrate deeper into coarse grained snow and the probability of absorption increases due to the multiple scattering in the snowpack. During melting most of the BC particles are assumed to accumulate near the surface due to inefficient runoff. Combined with more solar radiation, this results in a maximum radiative forcing during spring and summer. Finally, energy, in the form of latent heat, is needed to melt the snow. When there is less snow, the energy normally used during melting can warm the earth-atmosphere system instead. All these mechanisms act to enhance the warming effect from BC, and the ef-

ficacy of the BC/snow forcing is more than 3 times that of CO_2 [1] (Flanner et al., 2007).

2.3 Atmospheric transport

The spatial and temporal distribution of atmospheric components is determined by several processes, including surface emission and deposition, chemistry, and transport. Transport involves both large-scale advective motions (quasi-horizontal direction) and smaller scale processes such as convection (vertical displacement) and turbulence (Brasseur et al., 1999). The atmospheric circulation and wind patterns are a result of the uneven heating of the Earth's surface and following strong temperature gradients.

2.3.1 General circulation and global windpatterns

The general circulation of the troposphere is often described by a three-cell model, as illustrated in Figure 2.3. The Hadley cells, one in each hemisphere, are characterized by rapid lifting in the inter-tropical convergence zone (ITCZ), poleward transport in the upper troposphere, slow sinking in the subtropics and equatorward flow near the surface. As the air travels south again it gains a motion towards west due to the Coriolis force and forms the Trade winds, which dominate the horizontal transport. The Hadley cells cover large areas and the circulation is more vigorous during winter. The strong concvection around the Equator leads to frequent precipitation.

In the mid-latitudes, from 30° to 60°, the Ferrel cells dominate. The circulation in these cells is in the opposite direction from the Hadley and polar cells. Warm air travelling north meets cold air from the poles around 60° and is forced to rise above. As it rises, it cools and precipitation forms. Air flows southwards in the upper troposphere, and, because it is colder and heavier, sinks in the subtropics. The circulation is wave driven, a result of baroclinic disturbances. In these latitudes the westerly winds dominate horizontal transport. In the Northern Hemisphere there is also a much

[1] Efficacy is defined as the global mean temperature change per unit forcing produced by the forcing agent relative to the response produced by a standard CO_2 forcing (Hansen et al., 2005)

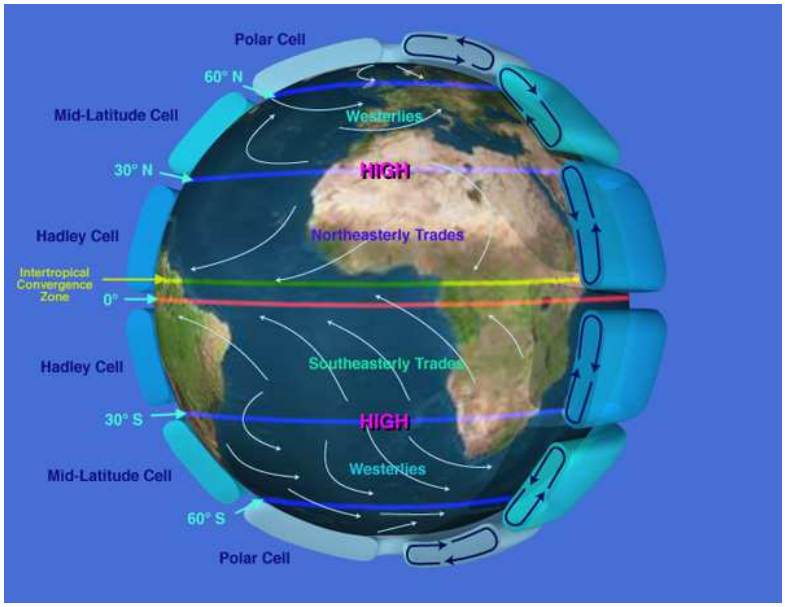

Figure 2.3: *Illustration of the global circulation cells and wind patterns (http://sealevel.jpl.nasa.gov/overview/climate-climatic.html).*

stronger seasonal difference in vertical motions. In winter, horizontal temperature gradients are strong, resulting in strong horizontal motions. During summer, stronger heating of the surface leads to increased vertical motion and also more efficient wet removal. Seasonal changes in the location of quasi-stationary pressure system also take place in the Northern Hemisphere.

The mean motion of the air is called the mean meridional circulation, and is represented by two large cells in the upper troposphere and lower stratosphere, one in each hemisphere. Air is lifted around the Equator and transported poleward aloft, followed by sinking as it reaches lower temperatures at the poles. Near the surface, the transport is directed towards the Equator again. Net transport of energy, moisture and pollutants is thus always poleward. In the stratosphere, there is only one meridional circulation cell that covers both hemispheres and changes direction with season.

2.3.2 Transport to the Arctic troposphere

As pointed out in Section 1, transport to the Arctic troposphere is impeded by the Arctic front. It is formed by surfaces of constant low potential temperature that form closed domes over the Arctic (Klonecki et al., 2003). The front is asymmetrical and can occationally be located far south. Because of this the Arctic troposphere was long believed to be very clean. In the 1950s, however, a phenomenon named the Arctic haze was discovered. The haze was initially thought to consist of ice crystals, but in the 1970s it became clear that it has anthropogenic origins, a fact that surprised many (Quinn et al., 2007). It was evident that pollution was transported this far north, but if an air parcel is to penetrate the Arctic dome, the air must have the same low potential temperature as these surfaces. For most Northern Hemisphere pollution sources the temperature is too high for direct transport. Transport to the Arctic lower troposphere therefore requires strong cooling of the air, which can be achieved through ascent or when air travels across cold snow covered surfaces (Stohl, 2006). Stohl (2006) characterized three paths for pollution transport into the Arctic:

1. Low-level transport followed by ascent in the Arctic. Requires the air to be already cold and dry, and is only possible for sources located north of the Arctic front.

2. Low-level transport alone. Involves transport over snow-covered surfaces.

3. Uplift outside the Arctic, often close to the sources, high-altitude transport and descent in the Arctic.

Pollution from Europe can follow all three paths in winter, and the first and third in summer. Pollution from Asia and North America can only follow the last pathway. Particles following the first route are important because they enter at low altitudes, followed by ascent, precipitation and wet deposition in the Arctic. Particles lifted close to their sources, as in the third transport route, generally go through several cycles of ascent and descent, increasing probability of wet removal outside the Arctic. The concentration of BC in the Arctic troposphere is highest during winter and spring, and is mainly from anthropogenic sources. Pollution concentrations are at a minimum during summer when transport is slower, temperatures higher and removal mechanisms more efficient. In the lower stratosphere, the potential temperature is even higher than in many source regions, and transport from the stratosphere to the Arctic troposphere is

small. In Stohl (2006) the probability of stratospheric transport is found to be less than 1% in winter and less than 0.1% in summer, while typical mid-latitude values are $1 - 10\%$. Stohl (2006) did not consider deposition of pollutants, but points out that if air is lifted, the probability of precipitation and removal of water-soluble species outside the Arctic increases. If, on the other hand, the air is cooled from the surface it is stabilized and the dry deposition decreases. Transport of particles are of course limited by their lifetime.

2.4 Lifetime and aging

The atmospheric lifetime of a component, τ, is the average time that a molecule of the species remains in the atmosphere, assuming no additional production or emission. It is determined by the inverse of the loss rate L:

$$\tau = \frac{1}{L}$$

The main loss of BC is through wet removal, with only a minor loss through dry deposition. As mentioned, most of the emitted BC is hydrophobic. Several models, including the Oslo CTM2, assume that the fractions emitted as hydrophobic and hydrophilic are 80% and 20%, respectively. Hydrophobic particles are not removed through precipitation and a key parameter determining the lifetime of BC is therefore the aging time. Slow aging means that BC is less efficiently removed, and the lifetime is increased. There are several processes through which particles are aged (Croft et al. (2005)):

1. Physical processes:
    - Condensation of sulphuric and nitric acid onto the BC aerosol.
    - Coagulation with more soluble species, such as sulphates.
2. Chemical processes:
    - Oxidation, which results in the formation of suface groups that can form hydrogen bonds.

Sulphate and sulphuric acid is produced by aqueous- and gas-phase oxidation of SO_2 by atmospheric oxidants such as OH and H_2O_2. These oxidants are produced by photochemical reactions, which require solar radiation. The aging of BC is thus determined by the amount of SO_2 and

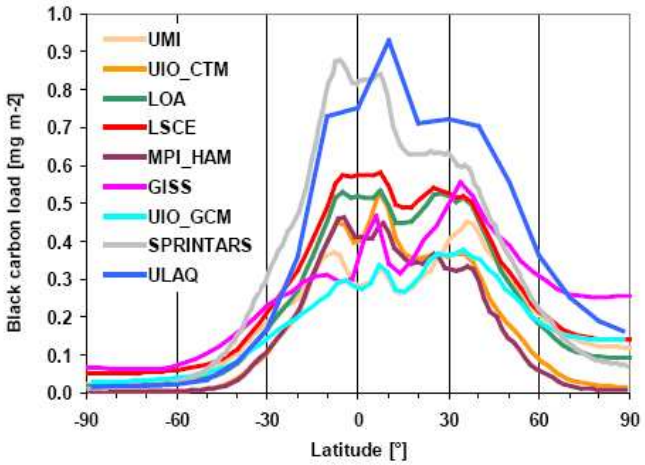

Figure 2.4: *Comparison of different model results for zonal burden of BC in mg* m^{-2} *(Schulz et al., 2006).*

oxidants available. This further affects lifetime because, described in Section 1, small emissions of SO_2 or lack of OH can increase BC lifetime by slowing down aging, thus reducing wet removal.

A study by Schulz et al. (2006) compares the lifetime and burden for different aerosol species from several global models. In this study, the BC lifetime ranges from 4.9 to 11.4 days, with an average of 7.3 days. The BC lifetime from the CTM2 model is 5.5 days, in the lower end of the interval. Figure 2.4 shows the zonal burdens from this work. Figure 2.4 will be compared to the burden calculated in this thesis in Chapter 4.

2.5 The cryosphere

There is a close connection between snow, ice and climate change. The cryosphere consists of all snow, sea ice, lake and river ice, ice sheets and ice shelves, glaciers and ice caps, and frozen ground. Presently, ice permanently covers 10% of the land surface, and about 7% of oceans in annual mean. During winter in the Northern Hemisphere, up to 50% of the surface can be covered with snow (Lemke et al., 2007). The cryosphere is the second largest component of the climate system, after the ocean, and

elements of it can be found at all latitudes. It has influence on surface energy and moisture fluxes, clouds, precipitation and circulation in the atmosphere and ocean. Fresh snow reflects up to 95% of the incoming solar radiation and is an important cooling factor in the climate system. All parts of this system contribute to short-term climate change. Permafrost, ice sheets and ice shelves also contribute to changes over a longer timescale, such as change in the cycle of ice ages.

Observations have revealed a global scale decline of snow and ice over many years. The latest IPCC rapport (Lemke et al., 2007) includes a summary of observed changes to the cryosphere, mainly from the 1960s and forward, and some of these are:

- Snow cover has decreased in most regions, and most noticeably in spring and summer.
- There has been a 2.7% decline per decade in annual mean Arctic sea ice extent since 1978, and satellite data reveal that this decline continues. Data from submarines also indicate that the thickness of the Arctic ice has very likely [2] decreased.
- There has been strong mass loss of glaciers and ice caps.
- The ice sheets of Greenland and the Antarctic has very likely been contributing to the sea level rise in the period 1993 to 2003.
- The maximum extent of frozen ground in the Northern Hemisphere has decreased by 7% from the beginning of the previous century.

Continuing changes in the cryosphere will have consequences for the environment and for humans (UNEP, 2007). Indigenous people who live in the traditional way, such as the Inuit and Samii, face major challenges, and the ecosystems in polar and mountainous regions will change. Sea level rise can affect the strenght of the major ocean circulation and cause problems for many Islands and coastal regions. Furthermore, decline in glaciers can lead to regional freshwater shortage, also affecting the aggriculture.

The cryosphere is affected by both natural variability in the climate system and external factors such as anthropogenic emissions. As described in Section 2.2, absorbing particles in snow pack and ice has a potentially strong warming effect. After the Arctic Haze phenomenon was discovered, meas-

[2]The term "very likely" is used when there is a 90% or more probability of an outcome

urements have revealed that BC is in fact transported to the Arctic and deposited there, and may therefore play an important role in the observed decreasing trend in the cryosphere. Many studies have focused on the effect of BC on the surface albedo and the radiative forcing (Hansen and Nazarenko (2004), Jacobson (2004), Flanner et al. (2007)). In addition, ice-core measurements can potentially shed some light on the historical concentration and sources. The understanding of the effects involved is, however, relatively low (Forster et al., 2007) and more research is necessary.

Chapter 3

Method

3.1 Model description

3.1.1 CTM2 model

The Oslo CTM2 model is a global 3-dimensional model for calculating the transport and distribution of chemical species in the atmosphere. Transport is driven by actual meteorological data from the European Centre of Medium Range Weather Forecasts (ECMWF), which is calculated off-line and updated every third hour. Input data includes information about temperature, pressure, humidity, precipitation and cloud coverage. The model has several options for horizontal and vertical resolution. The choices for horizontal resolution are $5.6\,^{\circ}x5.6\,^{\circ}$, $2.8\,^{\circ}x2.8\,^{\circ}$, $1.89\,^{\circ}x1.89\,^{\circ}$ and $1\,^{\circ}x1\,^{\circ}$. The vertical resolution is 19, 40 or 60 layers, with the first at the surface and the topmost at around $10hPa$. The layers are most closely spaced in the lower atmosphere. The model has separate modules for tropospheric chemistry, sea salt, dust, nitrate, sulphur, stratospheric chemistry, and black and organic carbon. It is possible to run the model with full chemistry, or with only some of the different modules. The different options are set by changing logical switches. The model includes the following dynamical and chemical processes:

- **Convective and advective transport** of the tracers, calculated every hour. The convection, vertical mixing, uses the Tiedtke mass-flux scheme (Tiedtke, 1989), while the advection is done with second-order moment method (Prather, 1986).

- **Dry deposition**. The deposition velocity depends on the thickness of the surface layer, the eddy diffusion, and the characteristics of the surface (land, ocean).
- **Wet removal**, large-scale and convective wet removal (Berglen et al., 2004).
- **Chemistry**. The chemistry scheme in the model consists of 51 tracers and 108 photolysis and chemical reactions for tropospheric chemistry (Kvissel, 2007). In the scheme, the mass balance equation

$$\frac{dC_i}{dt} = P_i - L_i * C_i$$

where P is production, L is loss and C is concentration for species i, is solved using the Quasi Steady State Approximation (QSSA) with a timestep of 15 minutes. The analytical solution when all production and loss terms are known is

$$C_i(t) = C_i(0) * exp(-\frac{t}{\tau_i}) + \tau_i * P_i(1 - exp(-\frac{t}{\tau_i}))$$

The first term on the right hand side is the decay of an initial concentration, while the second term represents the approach to steady-state. Quasi steady state means that the production rate is assumed to vary only on timescales longer than τ (Jacobs, 1999).

- **Boundary layer mixing**, mixing due to turbulence, is also done every 15 minutes. The boundary layer is an important part of the model because dry deposition and most of the emissions take place here.

3.1.2 BC in the original Oslo CTM2 aerosol parameterization

Emissions are updated at the beginning of each new month. BC is emitted as 80% hydrophobic and 20% hydrophilic. There are four BC components. BCFFPHOB and BCFFPHIL are hydrophobic and hydrophilic fossil fuel pluss biofuel emissions respectively [1], and BCBBPHOB and BCBBPHIL, which are the insoluble and soluble biomass burning emissions. Emission data for fossil fuel BC is taken from Tami Bond's work (Bond et al., 2006),

[1] Hereafter, the term fossil fuel BC is used as a generic term for BC from both these sources.

and is based on information about energy consumption in 1996. Monthly emissions from biomass burning are taken from the Global Fire Emissions Database version 2.1 (GFEDv2.1) for 2004. Total emission for this year is 2.7 Tg. Information about areas with fires and burned areas are taken from images from the Moderate Resolution Imaging Spectroradiometer (MODIS), which is an important instrument aboard satellites. Emissions are then calculated as a function of burned area, fuel loads and combustion completeness [2] (Randerson et al. (2007) and references therein). All emissions are originally gridded in $1\,^{\circ}x1\,^{\circ}$, and are then interpolated to match the resolution chosen. Due to the release of heat, and the following strong vertical lifting, biomass burning emissions are distributed through several layers. Fossil fuel is emitted only at the surface, but there is a diurnal cycle with 50% higher emissions during daytime. No chemistry is involved in the original version of aerosol parameterization. As described earlier, the BC particles are transferred to hydrophilic mode at a constant rate of 24% per day (Maria et al., 2004). The transfer rate is only an estimate of the aging time, not an accuarate calculation. It must be emphasized that a constant aging is not physically correct. The transfer rate can, however, be adjusted to improve model performance, as was done in the CTM2. The loss of hydrophobic aerosols happens through transfer to hydrophilic mode and by dry deposition. The hydrophilic particles are removed through both dry and wet deposition. Only in-cloud wet removal is parameterized. Particles are assumed to be completely absorbed in the cloud droplets, and are removed according to the fraction of the liquid water content of a cloud that is removed during precipitation (Berntsen et al., 2006).

The output from the model is three-dimensional fields for concentration for each month. It is also possible to have the concentrations written to file every third our. The concentration is given in volume mixing ratio, which is the ratio of the number density of the component to the number density of air. For aerosols it is more common to give the mass concentration, that is the mass per volume of air. Using the molecular mass of carbon and mean molecular mass for dry air, and the average density of air at sea level ($1200g\ m^{-3}$), the concentration of BC is given in ng pr m^3air in the surface distributions in Chapter 4.

[2] Combustion completeness depends on fuel type and moisture conditions.

3.1.3 The microphysical aerosol parameterization M7

As already mentioned in Section 1, many important aerosol characteristics are dependent on size and composition, such as the settling velocity, diffusion, optical properties and wet removal. A realistic representation of atmospheric aerosol includes not only total mass of a species, but also a size distribution and mixing state. The M7 aerosol microphysical module which is used in this work was originally design by Elisabeth Vignati (described in detail in Vignati and Wilson (2004)) and was recently coupled to the Oslo CTM2 by Alf Grini. Here, the module is described in more detail, and the description is based on Vignati and Wilson (2004) and Grini (2007). M7 describes the size distribution of sea salt, dust, sulphate and black and organic carbon with the lognormal distribution function. This function is expressed as

$$n(lnD_p) = \frac{dN}{dlnD_p} = \frac{N}{(2\pi)^{1/2} * ln\sigma_g} * exp[-\frac{(lnD_p - lnD_{pg})^2}{2ln^2\sigma_g}]$$

and descibes a Gaussian distribution with the logarithm of particle diameter on the x-axis. D_p is particle diameter, D_{pg} the geometric mean diameter, σ_g is the geometric standard deviation and N is the number concentration. In M7 aerosols are divided into two types of particles; mixed (water soluble) and insoluble. There are four size-classes; nucleation $\sim 1nm$, Aitken $\sim 0.01\mu m$, accumulation $\sim 0.1\mu m$ and coarse mode $\sim 1\mu m$. Different soluble particles can exist in all four modes, while the insoluble are divided into three modes (BC/OC insoluble Aitken, dust accumulation and dust coarse mode). This gives a total of seven modes to represent the whole aerosol population. The nucleation mode contains only sulphate. Due to their sizes, sea salt and dust are only represented by the two largest modes, and only dust can be present as insoluble. BC and OC can exist in insoluble Aitken mode and in soluble Aitken, accumulation and coarse mode. Each mode is represented by the total particle number and mass from which the average particle radius is calculated. Figure 3.1 illustrates the size distribution. Processes that can change the aerosol composition and size are:

- Condensation, gas condensing onto particles making it water soluble.
- Coagulation, growth of particles through collision or transfer to hydrophilic mode by collision of insoluble paticles with soluble species.
- Nucleation, formation of particles from gas phase molecules.

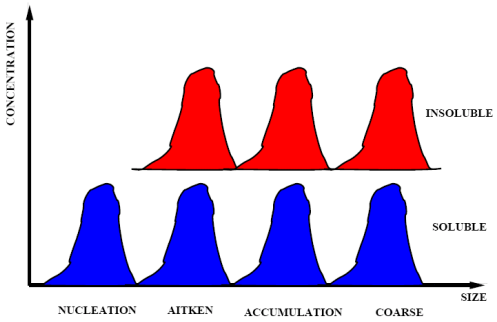

Figure 3.1: *Illustration of the lognormal representation of aerosol sizes, (Grini, 2007)*

When M7 is used, there is a change in the parameterization of dry deposition. In the original version of the Oslo CTM2, the deposition velocity is the same for all particles of a species. In M7, a scheme where deposition velocity also depends on particle size and density is used. Dry deposition is more effective for large particles.

In the M7 module four new components are used to represent BC; BCKS, BCAS, BCCS and BCKI, which are soluble Aitken mode, accumulation mode, coarse mode and insoluble Atiken mode. The emissions from Bond and GFED are still used, but there is no longer a separation between fossil fuel BC and biomass burning BC. Each time emissions are updated, all particles are put in the insoluble Aitken mode. When the particles are coated by a monolayer of sulphuric acid, i.e. a single layer, they are considered aged and are moved to the soluble Aitken mode. This happens through condensation, and only the sulphuric acid produced by the gas-phase reaction $OH + SO_2 \longrightarrow H_2SO_4$ can contribute to this process [3]. Insoluble particles are also aged through coagulation with other soluble aerosols. Coagulation and condensation increase the geometrical mean radius of particles. The modes in M7 are defined by fixed size intervals. When particles gain a radius larger than the upper limit of their mode, they are transferred to the next mode.

When M7 is applied, chemical processes determine the aging, and the CTM2 has to be run with modules for BC/OC, dust, sea salt, sulphur and tropospheric chemistry. This results in increased use of computer memory

[3]Sulphate produced through aqueous chemistry only contributes to increasing the mass of already soluble aerosols

and time compared to using only the BC/OC module. Running the model for one and a half years on four CPUs takes around nine days with the M7, compared to approximately one day with the original version. The choice of aerosol representation is easily changed with a logical switch, but it is important to change the input-file containing the atmospheric components, because the M7 requires several components which are not part of the original parameterization.

3.1.4 Modeling of BC in snow and ice

The routine which is used to model deposition and accumulation of BC in snow and ice was created by Ragnhild Skeie (Skeie, 2007) at Center for International Climate and Environment Research Oslo (CICERO). A maximum of ten snow layers are created using snow data from ECMWF, which is updated every three hours. If there is no additional snow fall during the next 24 hours after an initial snow fall, a new layer is created. The topmost layer is limited to a thickness of $1mm$. If there already are ten layers when a new one is created, the two at the bottom are merged. Dry deposited BC is included only in the thin layer at the top, while BC deposited through precipitation is included in the layer below as well. Data from ECMWF is also used to simulate melting and evaporation of the layers, and it is assumed that BC accumulates near the surface (in gridboxes with sea ice, no such data exists, and a constant melting from mid April to the 21st of June is assumed). The BC content in the snow column is conserved until the whole snow column is melted, at which point all BC is also removed. Output is written to file every third hours, and a file containing three dimensional fields for the snow layer in unit m of water equivalent and for biomass and fossil fuel BC concentration in $kg\ m^{-2}$, is created. When plotting the concentration of BC in the snow the unit is $ng\ g^{-1}$ and the concentration is averaged over the top three layers.

3.2 Model setup and experiments

The background for the experiments and simulations conducted in this work was described in Section 1. For this thesis, the CTM2 model is run with horisontal resolution of $2.8^\circ x 2.8^\circ$ and 40 vertical levels. First the model is run with only the module for black and organic carbon. When M7

Nr	Description
1	Standard simulation with the original aerosol representation
2	All wet removal of BC switched off
3	Convective wet removal of BC switched off
4	A subcloud scavenging added for the BC components
5	Standard simulation with M7
6	Same as 2, but with M7
7	Original aerosol representation with the snow/ice deposition routine included
8	Same as above, but with emissions only in China
9	Same as above, but with emission only in Europe
10	Simulation with M7 and the snow/ice deposition routine
11	Same as above, but reduced emissions of BC in China
12	Same as above, but reduced emissions in Europe
13	Simulation with increased emission of SO_2 in Europe

Table 3.1: *Overview of simulations done with the CTM2 model in this thesis.*

is used, tropospheric chemistry as well as sulphure, dust and sea salt aerosols is included. All simulations are for the period $1/1-05$ to $30/6-06$, with the first 6 months as spin-up. In addition to standard simulation with and without M7, and simulations with deposition of BC in snow and ice with the two parameterizations, several sensitivity simulations for wet removal are done. This work also includes regional experiments as described below in Section 3.2.3. Table 3.1 summarizes the simulations conducted in this work.

3.2.1 Subcloud scavenging

As part of the work with the thesis, a routine for subcloud scavenging of BC was made and included in the model. This was done using the same equation and parameters as in the sulphur module (Berglen et al., 2004). The scavenging is given by

$$Q_{sub} = C * m_p * E_m$$

according to Berge (1993). Here m_p is the precipitation mass in $kg\ m^{-3}$, $C = 5.2 m^3 kg^{-1} s^{-1}$ and $E_m = 0.1$ is the mean collection efficiency. It is assumed that 20% of the cloud in a gridbox is precipitating.

3.2.2 Including the M7 in the snow and ice routine

For the first time with the Oslo CTM2 model, the deposition of BC on snow and ice covered surfaces is modeled with the M7 aerosol parameterization. Hence, an important part of the work with this thesis was to change the deposition routine so it could be used in combination with M7. This was done to investigate the effect of applying the new aerosol parameterization on BC concentration in snow and ice. The main structure of the routine remained unchanged, but the description of deposition and concentration of BC had to include all four M7 BC components. All variables related to BC was extended to account for this. The dry deposition also had to be slightly changed for M7. Due to the linearity in the original aerosol parameterization the equation

$$\Delta C = C_0(1 - exp(-\Delta t * L))$$

which describes loss of BC without any additional emissions, could be approximated by

$$\Delta C = C_0 * \Delta t * L$$

With the M7 module the exact equation is kept to avoid any errors caused by non-linearity. The output file was also extended to include a field for each of the four new components in addition to the snowlayer field.

3.2.3 Emission regions

In order to study regional differences and contributions, simulations with two emission regions are done. The definition of Europe and China is shown in the map in Figure 3.2. For simulations with the original parameterization, emissions from all other areas than Europe or China are excluded. This can be done because of the simple linear transfer rate from hydrophobic to hydrophilic mode. Thus, contributions are from a 100% of fossil fuel BC emissions in the region. The particle interaction in M7 means that aging and growth is dependent on the transport of pollutants into the region of interest from surrouding gridboxes. Therefore, emissions in the surrounding gridboxes cannot simply be set to zero. Instead, emission of BC from fossil fuel use are reduced by 20% in each of the regions. Biomass burning emissions are much more difficult to address by regulations, so they are not changed here. The resulting contributions with M7 are scaled by a factor five to match a 100% reduction. In the final sensitivity experiment, emissions of SO_2 is increased with 70% in Europe. This is done only

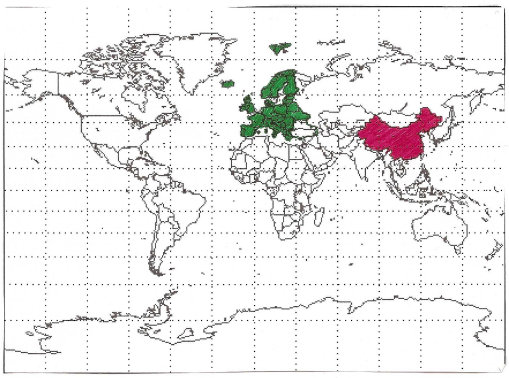

Figure 3.2: *Regional experiments were done with emissions from Europe (green) and China (red).*

for the industry and power plant sector, which are the sectors where most of the reduction in the past decades have taken place.

Chapter 4

Results

4.1 Original aerosol parameterization

4.1.1 Surface distribution

Figure 4.1 shows the annual mean concentration of total BC in the lowest layer of the model in $ng\ m^{-3}$. The concentration is high over most of the continents with values over 250 $ng\ m^{-3}$. Maximum values are found close to the major emission regions, reaching $1 - 3\ \mu g\ m^{-3}$. There is little BC south of $60\,^{\circ}S$ because of the large areas with no emission sources and the short lifetime of the particles. One can see the cross-Atlantic transport with the Trade winds from central Africa, and also the eastwards transport from China and North America, as well as Europe. Concentrations in the Arctic are less than 10 $ng\ m^{-3}$. The short lifetime of BC is seen from the rapid decrease in concentration away from the main sources. Annual global lifetime is calculated as

$$\tau = \frac{Annual\ mean\ burden\ [Tg]}{Global\ sources\ [Tg\ yr^{-1}]}$$

With the original aerosol parameterization, annual mean burden is 0.17 Tg and BC lifetime is 7.63 days. This is close to the mean value in the study by Schulz et al. (2006). The lifetime found here is longer than the 5.5 days from the CTM2 results in that study. This is due to the lower transfer rate which is used now, leading to less wet removal of BC.

Figure 4.2 shows the seasonal variation in BC concentrations, again in the

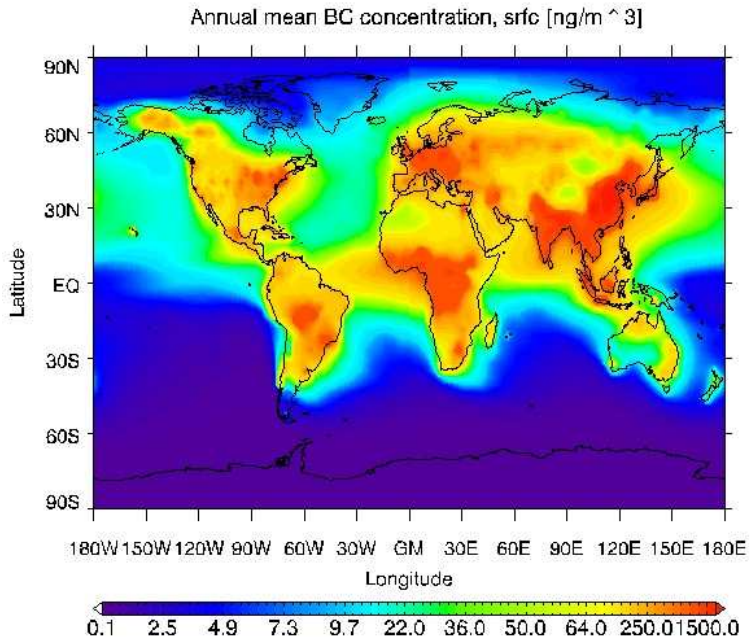

Figure 4.1: *Annual mean concentration of BC in the lowest model layer with the original aerosol parameterization, [ng m^{-3}].*

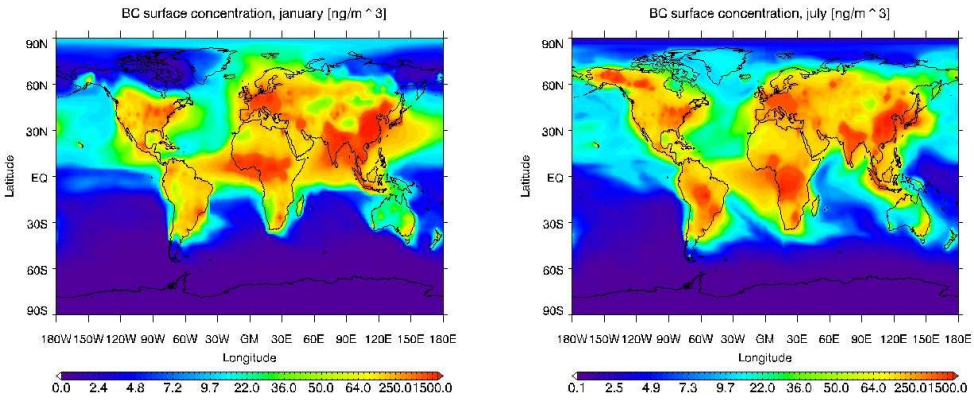

(a) January (b) July

Figure 4.2: *BC concentration in the lowest model layer with the original aerosol parameterization in (a) January and (b) July, [ng m^{-3}].*

lowest model layer. Since there is no chemistry involved in this parameterization of BC, the seasonal differences in surface distribution arise from changes in meteorological and dynamical conditions, and differences in emissions. In mid-latitudes, concentrations off the coast from the main source regions are generally lower in the summer than in winter. This is likely caused by stronger horizontal winds and less efficient wet removal during winter. The difference is especially large in east Asia, but can also be seen in southern parts of Africa and South America. A strong seasonal difference can also be seen in the Indian ocean due to the monsoon. Lower concentrations over Greenland, Alaska and Northeast Siberia in January are most likely due to missing sources of BC from forest fires at this time of the year. The higher concentrations found in the Arctic troposphere between $60\,^{\circ}E$ and $60\,^{\circ}W$ in winter can be a result of less efficient wet removal in Europe and Russia. In addition, emissions from Europe can, according to the theory in Section 2.3.2, be transported to the Arctic via three paths in winter.

Modeled surface concentrations agree well with the results in Koch et al. (2007), except for north of $70\,^{\circ}N$ where their values are between 50 and 60 $ng\ m^{-3}$. Annual mean concentrations from the CTM2 at different locations (Table A.4) are also compared to concentrations modeled with the GATOR-GCM (Gas, Aerosol, Transport, Radiation, General Circulation and Mesoscale Meteorological model) in Jacobson (2002), and to observed annual mean values summarized in the same article (Tables A.1 and A.2). The CMT2 results are generally lower than both observations and concentrations modeled by the GATOR-GCM, especially at many of the marine and rural locations. At several of the urban sites, values from the CTM2 and the GATOR-GCM are in good agreement, but both models are unable to reproduce the large observed concentrations. This is very clear for Beijing, where observations show concentrations of up to 10000 $ng\ m^{-3}$, while modeled values are less than 1000 $ng\ m^{-3}$. Observations in Beijing are from 2001, and since estimates show that BC emissions increase in Asia, it is possible that the older emission data used in the model is too low. The decreasing trend in BC emissions in Europe could explain the much lower concentrations from the CTM2 model in Halle, Hamburg and Kap Arkona. Here, both observations and the data used in Jacobson (2002) are older that the data in the CTM2 model. One problem is that the resolution in the CTM2 simulations is relatively coarse. The values used for comparison are from the centre of each gridbox, and the location may therefore not correspond exactly to the location of measurements. Since BC shows a large variability in time and space, the concentration vary within each

Height	**Density of air [$g\ m^{-3}$]**	**Concentration of $1ppb$ in $ng\ m^{-3}$**
0 km	1225	507
5 km	736	305
10 km	414	171

Table 4.1: *Relationship between mixing ratio and mass concentration for BC in different atmospheric levels using standard values for air density*

gridbox, and this leads to uncertainties when comparing observations and modeled concentrations. Differences in meteorological conditions can also lead to some discrepancies for a short lived component such as BC.

4.1.2 Vertical distribution

The zonal means for fossil fuel BC and biomass burning BC in January and July are seen in Figures 4.3 and 4.4. Here, the amount of BC is given in volume mixing ratio, not in $ng\ m^{-3}$ as in the surface distributions. The mass concentration of BC in $ng\ m^{-3}$ corresponding to $1ppb$ is not constant with height due to the decreasing density of air. Therefore, to study the changes in concentration caused by transport and removal, not by the difference in density, the volume mixing ratio is kept. To give a feeling of the mass concentrations in the vertical distributions, Table 4.1 shows how many $ng\ m^{-3}$ $1ppb$ of BC corresponds to in three different altitudes using standard atmospheric values for density.

Fossil fuel BC has maximum values near the surface around $30\,^{\circ}N$, coincident with the major sources in Asia. For fossil fuel BC there is a strong seasonal difference in high altitude concentration due to much stronger vertical motions in the summer. This difference is smaller in the tropics where solar insolation is relatively constant, as can be seen in Figure 4.4. Biomass burning BC has maximum values around the Equator, again close to sources. The local maximum around $60\,^{\circ}N$ is due to forest fires in Canada and Eurasia, and, as also seen in Section 4.1.1, it is lacking in the winter when these areas are mostly snow covered. Biomass burning BC is more concentrated in the vertical than the fossil fuel components. Around the Equator the deep convection is strong, but the washout is also efficient and the particels are less dispersed. In addition, fossil fuel sources are spread over more latitudes than the main biomass burning sources. The efficient wet removal in the Hadley cell can be seen in the strong decrease in concentration from the Equator to approximately $30\,^{\circ}$, where the air is

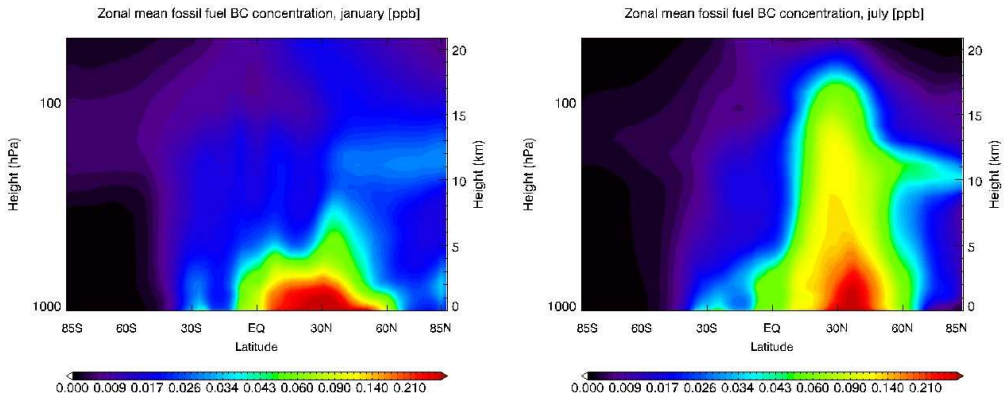

(a) January (b) July

Figure 4.3: *Zonal means of fossil fuel BC, sum om hydrophobic and hydrophilic component, with the original aerosol parameterization, [ppb].*

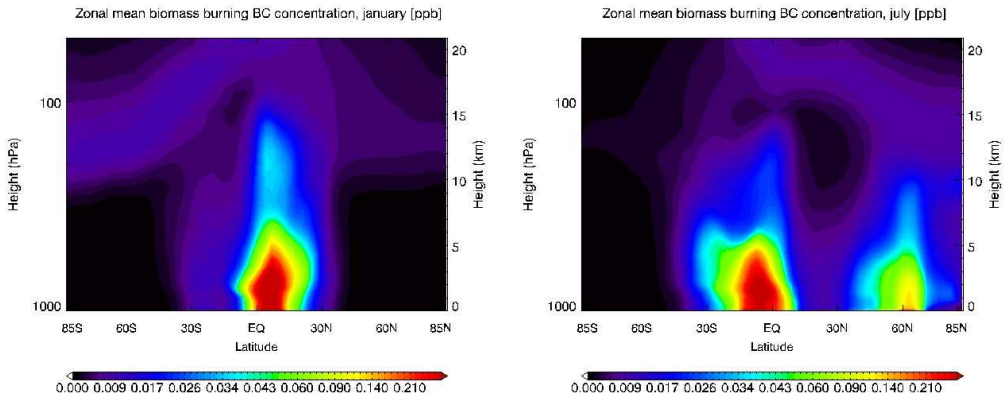

(a) January (b) July

Figure 4.4: *Zonal means of biomass burning BC, sum of hydrophobic and hydrophilic BC, with the original aerosol parameterization, [ppb].*

dry and sinking. Because of the short lifetime and efficient removal, the net poleward transport of BC by the mean meridional circulation is small, but can be seen for example in Figure 4.4(a). As can be seen in Figure 4.3(b) and 4.4(b), the Antarctic troposphere is extremely isolated during winter.

4.1.3 Transport and wet removal

The importance of wet removal as a loss for BC can be seen in Figure 4.5, which shows the percentage difference in BC concentration between a simulation without wet removal and the control simulation with original wet removal. Small values means that washout is not yet important, while higher values show where more BC is removed in the control simulation. Switching the wet removal completely off is, of course, a purely hypothetical test. It can, however, be used to study the potential for transport of BC, since values less than 100% show regions where BC is not yet removed by wet removal and can be transported from. Differences less than 50% are only found close to the emission sources and we see that most BC is removed close to the sources, again illustrating the short lifetime. In remote areas the difference is close to 100%, indicating that little BC is transported here. The dry deposition is the same in both simulations, so the large difference also shows that dry deposition is only minor loss mechanism for BC. The most obvious seasonal difference can be seen for fossil fuel BC over India and the Indian Ocean. In July, transport from India is even more limited than in January. This is a result of the monsoon. In summer, land heats up and the rising air is being replaced by warm, moist air from the ocean which then is forced to rise when meeting the Himalayas. The strong increase in precipitation in this season removes more BC. In winter, cold, dry air blows from the north towards Equator and the BC transport over the Indian Ocean increases by nearly 50%.

Hydrophilic BC is lost through large-scale and convective wet removal. To study the contribution from each of the two, the convective washout was switched off. Figures 4.6(a) and (b) show the difference in concentration between the simulation with only large-scale wet removal and the simulation with both processes (in per cent). This figure is for the sum of the hydrophilic BC components. The large-scale wet removal clearly provides the main contribution to the loss of BC. In most of the world convective precipitation contributes less than 20%. In general, convective precipitation is of little importance in Northern Hemisphere continental areas in

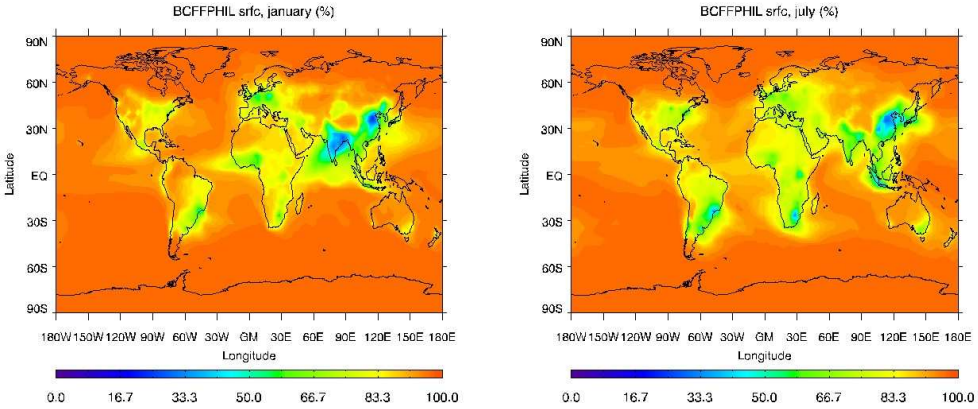

(a) January (b) July

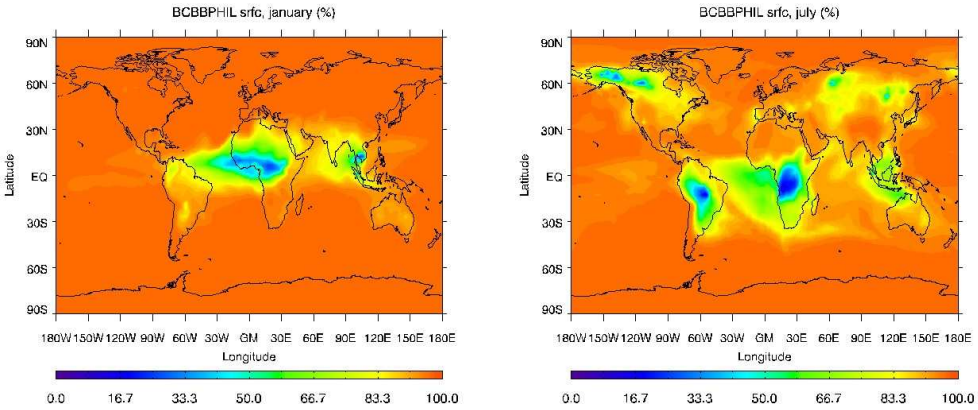

(c) January (d) July

Figure 4.5: *Difference in concentration in the lowest model layer between simulation without and with wet removal, with the original aerosol representation. Hydrophilic fossil fuel BC (top) and hydrophilic biomass burning BC (bottom), (%). Values less than* 100% *show regions where BC is not yet removed by precipitation and can be transported from.*

winter, consistent with weak vertical motions. In the Antarctic, the extremely low temperatures lead to a stable and dry atmosphere with close to zero contribution from convective precipitation. The only siginificant contributions are found over tropical oceans, where the vertical motion is strong and deep convection is frequent. During summer, the convective precipitation has a larger contribution over Eurasia, while during winter the contribution in the North Atlantic is stronger. This is consistent with the seasonal change in the pressure system; the low pressure is now over Siberia, while the Icelandic low is replaced by a high pressure system. In January, the maximum contributions from convection are found slightly farther south than in the summer, showing the seasonal movement of the ITCZ.

In the Oslo CTM2 model only the BC included in cloud droplets is removed during precipitation. In reality, rain drops can also collide with and collect particles as they fall, providing an additional loss, so-called subcloud scavenging. A parameterization for subcloud scavenging was tested in the model. Figure 4.6(c) displays the annual mean contribution of subcloud scavenging to the total removal of BC. Here, the difference in concentration in per cent between a simulation with original removal and one including subcloud scavenging is shown . The subcloud scavenging is negligible for BC, with only a minor contribution in some areas of up to 0.5%. As described in Section 3.2.1, the same parameterization as for sulphur was used. Berglen et al. (2004) found that the contribution of subcloud scavenging to the total removal is 1.3% for SO_2 and 0.1% for SO_4^{2-}, in the same range as for BC. There may be some uncertainty related to the use of the exact same equation. In addition, the collection efficiency used here (0.1) may be too low. Magono et al. (1979) found that snow crystals are efficient scavengers with a collection efficiency reaching unity for aerosols in the size range $0.1 - 0.5\ \mu m$, and Croft et al. (2005) used an efficiency of 0.3 in all areas in their parameterization. However, assuming a linear relationship, increasing the collection efficiency from 0.1 to 1 would increase maximum contribution to 5%, which is still negligible compared to the other removal mechanisms.

From the results above it can be seen that large-scale wet removal is the main loss for BC particles and most of the loss happens relativley close to the sources, indicating little transport of BC to remote regions. Convective precipitation stands for more than half of the total wet removal over oceans in tropical areas. Subcloud scavenging of BC is negligible even with a collection efficiency near unity.

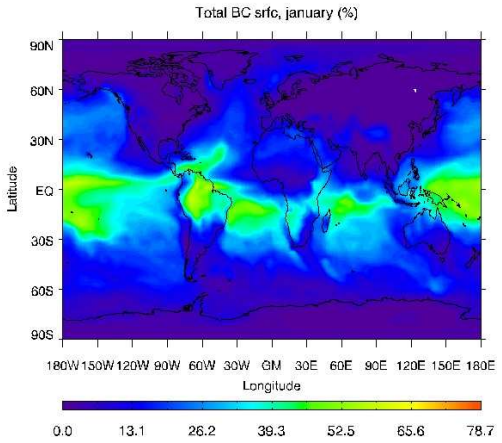

(a) Convective removal, January

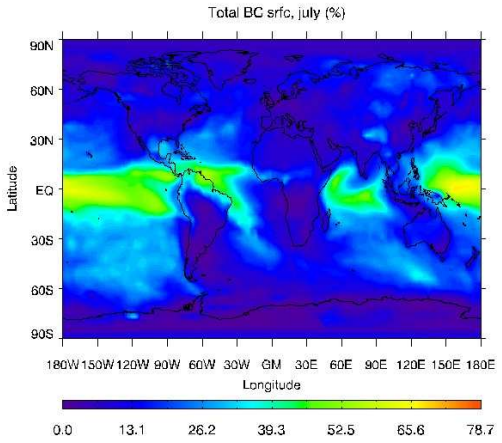

(b) Convective removal, July

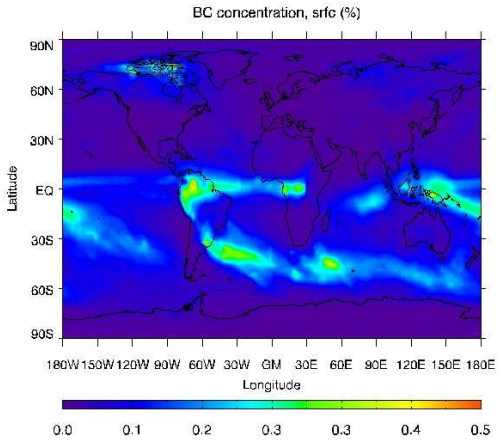

(c) Subcloud scavenging

Figure 4.6: *Percentage contributions to wet removal with the original aerosol parameterization; (a) from convective precitpitation in January, (b) from convective precitpitation in July, (c) annual mean contribution from subcloud scavenging.*

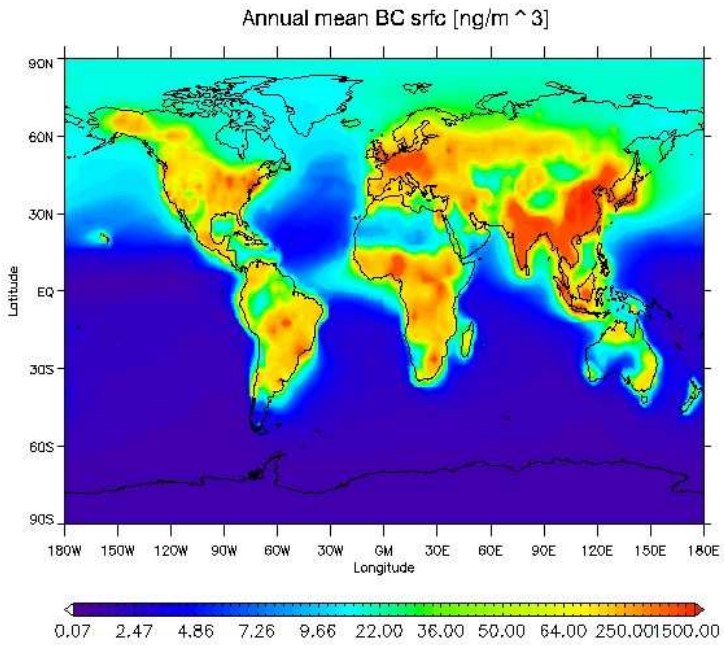

Figure 4.7: *Annual mean concentration of BC in the lowest model layer with the M7 module, [ng* m^{-3}*].*

4.2 M7

4.2.1 Surface distribution

When using the M7 module, BC distribution and its seasonal variation becomes a function also of chemical processes. Figure 4.7 shows the annual mean near-surface concentration of BC when the M7 module is used, and the seasonal concentrations are shown in Figure 4.8. The pattern in the annual mean concentrations is the same as in Figure 4.1 for the original simulation, and values in continental and source regions are comparable. However, there is more BC in high latitudes in the Northern Hemisphere. With M7, there is a strong seasonal difference in BC concentration north of $40 - 50\,^{\circ}N$, presumably due to different aging times. During winter, lack of sunlight reduces the oxidizing capasity of the atmosphere (less production of OH), and this reduces the amount of H_2SO_4 produced. Thus less BC is transferred to hydrophilic mode and can be removed than with the original parameterization, and the lifetime increases. More particles can be transported north, giving the increased concentration. The increase oc-

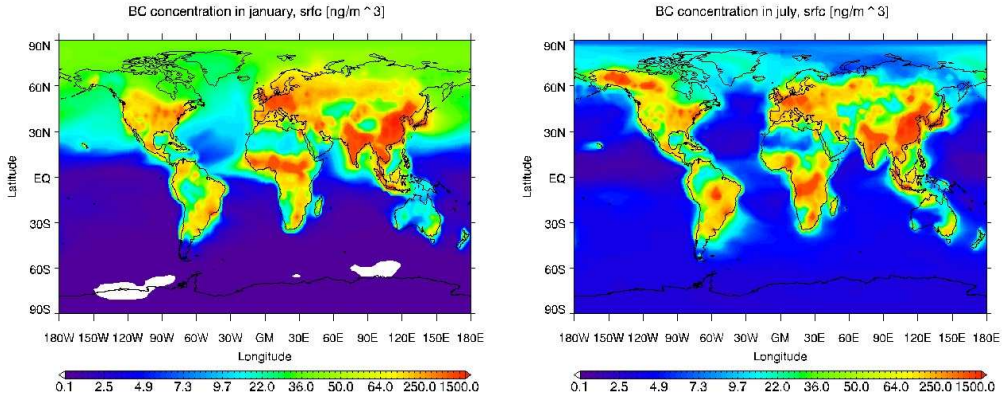

(a) January (b) July

Figure 4.8: *BC concentration in the lowest model layer with the M7 module in (a)January and (b)July, [ng m^{-3}].*

cur despite the lacking sources of BC in Canada and Eurasia, which in the original model version lead to a decrease in near surface concentrations in winter. Concentrations with M7 during summer are more similar to the original results. Aging is faster than in winter, and the aging time is also more similar to using constant transfer. The same seasonal difference can be seen in the Southern Hemisphere, with higher concentrations in July. In lower latitudes with more constant insolation, between 30 °S and 30 °N, the BC concentration decreases even more rapidly away from source regions than originally. Annual mean concentrations off the coast of East Asia and Africa, and over the Indian Ocean are reduced from between 40 and 200 $ng\ m^{-3}$ in the original version to between 10 to 40 $ng\ m^{-3}$ with M7. Concentrations over North Africa and the Middle East are also reduced. Particles are therefore removed more efficiently and closer to the source regions with the M7, and this is caused by a faster BC aging in these areas in both seasons. The global annual lifetime calculated here is 7.3 days and the global burden is 0.14 Tg, which is comparable to values in the original version.

The meteorological data is exactly the same as in simulations with the original version, and the effect of seasonal differences are again evident. The concentration of BC off the coast of East Asia and Central Africa is again lower in July than in January, and the difference is even larger than in the original version. There is still a seasonal difference in concentration

caused by the Indian monsoon, but it is less marked here than in Figure 4.2. This is probably because a more rapid transfer to hydrophilic mode occurs, which means a larger fraction of BC can be removed by the precipitation available in January, reducing the effect of the monsoon.

The results from the CTM2 with M7 are also compared with concentrations in Koch et al. (2007). There is now better match between their results and the concentration modeled here in January at high northern latitudes, but annual mean surface concentrations modeled by the CTM2 (Figure 4.7) at these latitudes are still lower than their results. M7 leads to a further underestimation of BC concentrations compared to measurements and values calculated by Jacobson (2002).

In summary, BC lifetime appears to increase in high latitudes, especially during winter, while there is a decrease in the tropics and subtropics close to source regions in both seasons compared to the original version. This is due to differences in aging. The global mean lifetime is 7.3 days, which is only slightly shorter than in the original parameterization. All BC particles are emitted as insoluble with M7, and the transfer of an extra 20% compared to the original version may also increase the lifetime. In general, seasonal differences in concentrations appear to be larger when M7 is applied as there are now three factors involved. An important consequence of having the mixed BC particles in the atmosphere is a stronger positive direct radiative forcing. Scattering material increase the probability of absorption due to multiple scattering, and Myhre et al. (2008) found an increase in the global mean direct radiative forcing of BC from $+0.26\ Wm^{-2}$ to $+0.33\ Wm^{-2}$ with coated particles. In theory, BC also has a stronger warming effect over high albedo surfaces, but the effect here is small because most of the increase in near-surface concentration in the Arctic occur in winter when sunlight is absent.

Table 4.2 summarizes global BC burden and lifetime with the two aerosol parameterizations and Figure 4.9 shows the annual mean ratio of the burden with M7 to the original burden in per cent. The burden with M7 is larger in high latitudes, while it is up to 40% lower in the belt between $60\,^{\circ}N$ and Equator. This is again seen in the zonal distribution of annual mean BC burden in Figure 4.10. The dot-dashed line shows the burden with the original version and the solid line is with M7. The pattern remains the same, but the subtropical maximum is underestimated with M7. Also these changes in burden are consistent with a slower BC aging in high latitudes and a faster transfer to hydrophilic mode in lower latitudes. The

Parameterization	BC burden [Tg]	BC lifetime [days]
Original	0.17	7.63
M7	0.14	7.3

Table 4.2: *Summary of global annual BC burden and lifetime with M7 and original version.*

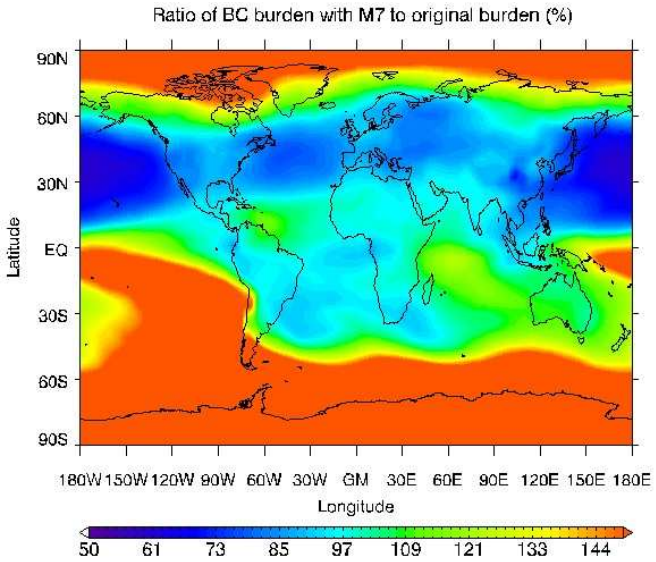

Figure 4.9: *Ratio of burden with M7 to burden with the original version (%).*

zonal burden from results in this thesis is compared to the results from Schulz et al. (2006) in Section 2.4. There are large discrepancies between the different models compared in Schulz et al. (2006), and the burden calculated here appears to be in the upper range. The burdens agree best with the results from the general circulation model LSCE, shown by the red line. There is, however, not a good match between the result from the CTM2 model in that study and in this thesis. As already pointed out, the transfer rate for BC has been adjusted, and this was done after Schulz et al. (2006) was published. We see that the effect of using a lower transfer rate is an increased burden, especially around $30\,^{\circ}N$.

Improvement?

We know that a constant BC aging is not realistic, and that M7 gives a more physical representation. As expected, using M7 results in regional

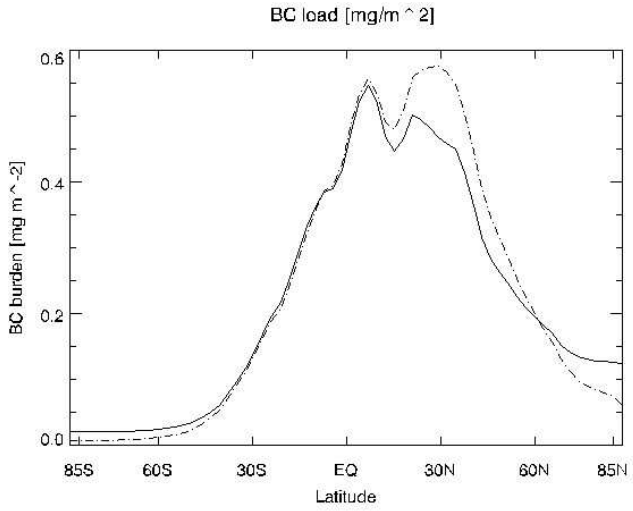

Figure 4.10: *Zonal distribution of BC burden in [mg m^{-2}], with the original model version (dot-dashed line) and with M7 (solid line)*

and seasonal differences in aging, and based on theory these results are not unrealistic. The M7 module does, however, introduce new uncertainties, such as the coagulation algorithm and assumption that one layer of sulphuric acid is sufficient to form a mixed particle. Vignati and Wilson (2004) tested the formation of mixed BC particles with M7 against a sectional model called AERO3. This test revealed that aging through coagulation alone is slower than in AERO3, while condensation gave a faster transfer. If condensation is in fact too fast in M7, it is possible that the BC concentrations modeled in lower latitudes are too low. This is supported by the fact that M7 leads to a further underestimation compared to Tables A.1 and A.2. Furthermore, the effect of reducing the transfer rate in the CTM2 to improve model performance, is most evident around 30 $^{\circ}N$. Using M7 reduce the BC concentration again in exactly this area. The BC burden with M7 increases relative to the original version in high latitudes, but with few observations to compare with, it is difficult to say if this is more correct. However, since aging indirectly depends on solar radiation, it is not unrealistic that concentrations can in fact be higher during winter.

4.2.2 Vertical distribution

Figures 4.11 to 4.14 show the zonal mean concentration for the four M7 BC components. The concentration of soluble Aitken mode BC is less than 0.03 ppb, which shows that particles grow rapidly to the next mode. Most BC resides in the accumulation mode, which can also be seen from the surface concentration if each component is displayed separately (not shown here). Accumulation mode BC has maximum values near the surface around source regions, which shows that aging and growth happens rapidly after emission. The concentration between 60 to 85 $^{\circ}N$ in January is very low, caused by the lacking emission sources and, more importantly, by the slower transfer from hydrophobic mode during winter. This can be seen by comparing with insoluble Atiken mode BC in the same latitudes in Figure 4.11(a). Here, concentrations are higher in the whole Arctic region. The concentration in accumulation mode decreases strongly with height and latitude, indicating that the lifetime in this mode is short. In M7 there is also an additional loss of these particles through transfer to coarse mode. The main concentrations of coarse mode BC is found over Sahara, the Middle East and Asia (seen from surface distribution of coarse mode, not shown here) where there are large dust particles to collide and coagulate with. The concentration of coarse mode BC is much smaller than for the other modes; values in Figure 4.14 are in ppt. Few particles grow into this domain, and those that do are efficiently removed.

Insoluble Aitken mode BC has a distribution that differ from the other components. The maximum concentration is around $0.1ppb$. During winter, the highest concentrations are found in lower levels in the Northern Hemisphere. This is because aging is slower and convection is less efficient. We now see that the increased near-surface concentrations in the Arctic in Figure 4.8(a) consists mainly of insoluble particles from fossil fuel sources. In July, the vertical motions are clearly stronger. The maximum concentration is found between 10 and 15 km around 30 $^{\circ}N$, and there is a local high altitude maximum over the Equator. In the atmosphere, strong convection can lift particles from the surface to high altitudes in one step. If particles had to be transported through one layer at the time, aging and following wet removal would lead to a decrease with height. The maximas show that the model representation of convection is realistic. Significant amounts of BC reach levels where the lifetime is longer, and where the warming effect may be stronger due to the underlying reflective clouds. The vertical distribution is important in the calculation of BC radiative forcing, and this result may therefore be important. Fast aging results in lower concentra-

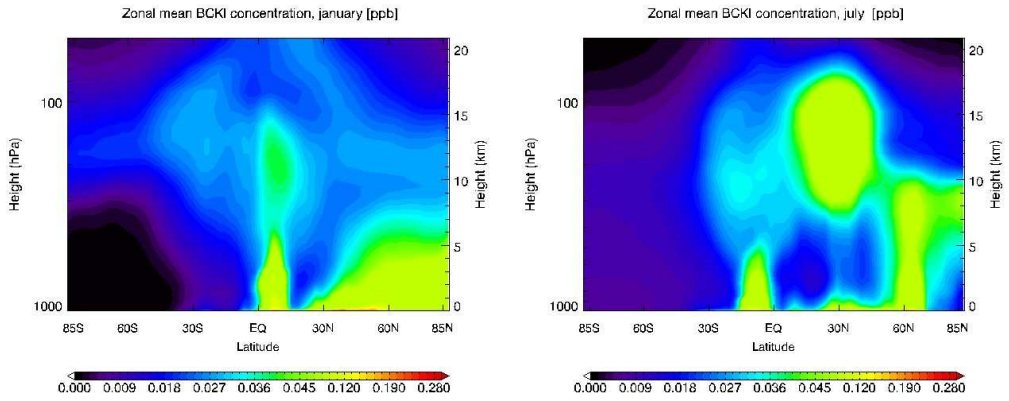

(a) January (b) July

Figure 4.11: *Zonal mean concentration for BC in insoluble Aitken mode in (a) January and (b) July, [ppb]*

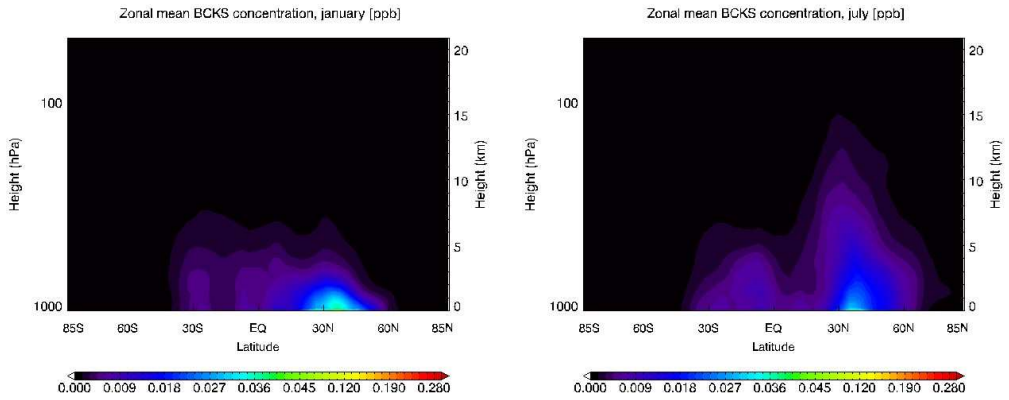

(a) January (b) July

Figure 4.12: *Zonal mean concentration for BC in soluble Aitken mode in (a) January and (b) July, [ppb]*

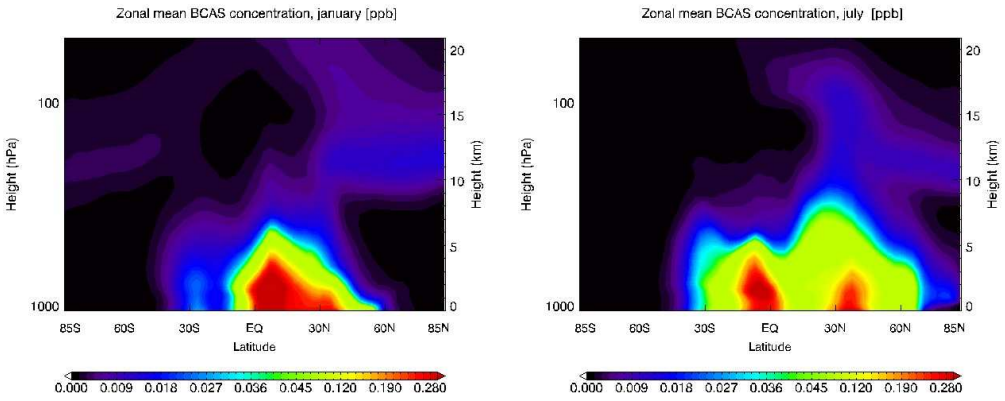

(a) January (b) July

Figure 4.13: *Zonal mean concentration for BC in accumulation mode in (a) January and (b) July, [ppb]*

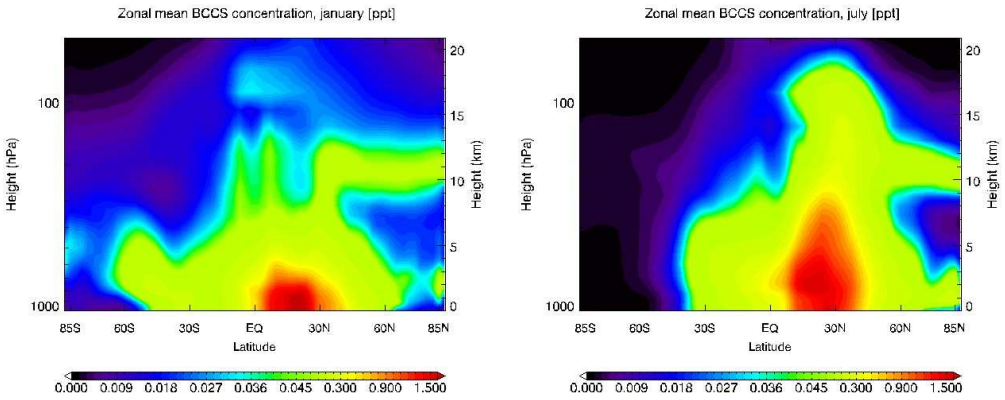

(a) January (b) July

Figure 4.14: *Zonal mean concentration for BC in coarse mode in (a) January and (b) July, [ppt]. Note the different unit.*

tion closer to the surface. Insoluble Aitken mode BC can be transported farther than the other components, which is seen from the higher background concentrations.

4.2.3 Transport and wet removal

As for the original BC components, a simulation to test the importance of wet removal is conducted. Figure 4.15 shows the resulting difference in surface concentration in per cent. For soluble Aitken mode BC, the difference is less than 50% in all regions. Looking back at Figure 4.5, where the maximum difference is close to 100% in large areas, it is clear that wet removal is not the main loss of Aitken mode BC. Most BC is lost through growth and transfer to accumulation mode. The white areas are regions with small negative values, meaning that concentration in the simulation without wet removal must be lower. It is possible that these values are simply caused by the non-linearity in M7. Another possibility is that switching off wet removal results in an initial increase in BC in the soluble Aitken mode. More particles can grow to accumulation mode, and the final concentration becomes lower than in the control run. For accumulation mode BC the pattern and values are more similar to those for the original components, with maximum values of to 100% in remote areas and small values close to the main sources where wet removal has not yet happened. Differences of $50 - 60\%$ are found over larger areas than with the original parameterization , which illustrates that growth is a loss for BC particles in this mode as well. Finally, for coarse mode BC the difference is always in the top 20%, indicating little potential for transport for these large particles, i.e most is removed close to the sources.

4.3 Regional contributions to atmospheric BC

This section focuses on the contributions to total zonal mean BC concentration and zonal burden from fossil fuel emissions in China and Europe, with the main focus on the region north of $60\,^{\circ}N$. As already mentioned, there have been several studies of regional contributions to BC in the Arctic atmosphere. Koch and Hansen (2005) found that $30 - 50\%$ of BC in the upper troposphere originate from Asia. At lower altitudes in spring, they found equal contributions of $20 - 25\%$ from Russia, Europe and Asia. These results were confirmed by Koch et al. (2007). Stohl (2006), however,

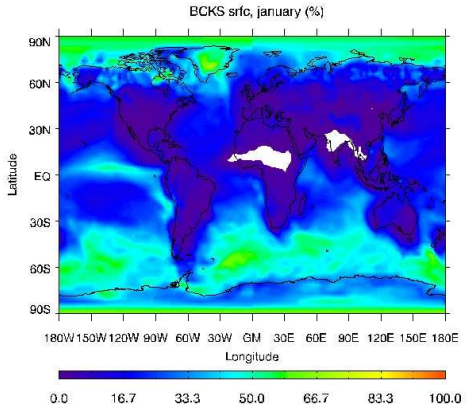

(a) BCKS, January

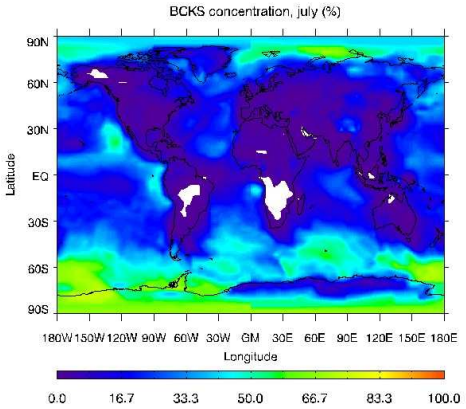

(b) BCKS, July

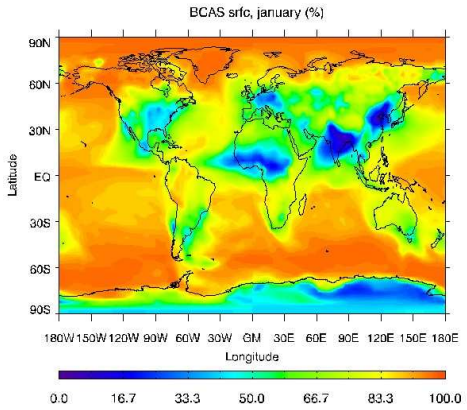

(c) BCAS, January

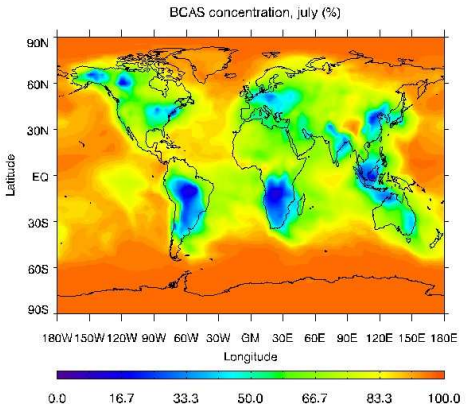

(d) BCAS, July

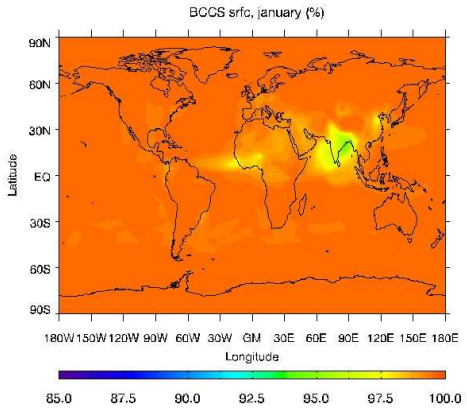

(e) BCCS, January

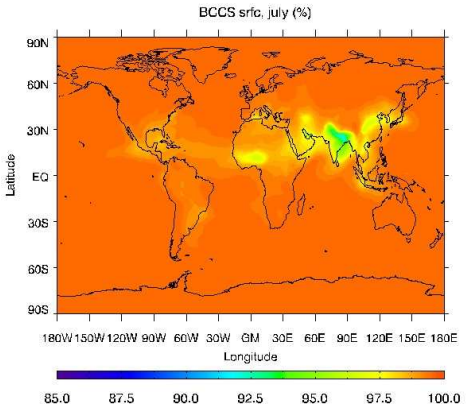

(f) BCCS, July

Figure 4.15: *Percentage difference in concentration in the lowest model layer between simulation without and with wet removal with M7. In January and July for BC in soluble Aitken mode (top), in accumulation mode (middle) and in coarse mode (bottom)*

found that European emissions are much more important, especially in the lower troposphere. His calculations showed that 75% of the particles originating from Asia need more than 14 days to enter the Arctic troposphere. This is twice as long as the estimates of BC lifetime in this thesis. Meanwhile, the fastest particles from Europe and Eurasia enter the Arctic in less than four days. These are also the particles with the highest probability of deposition in the Arctic. Stohl (2006) argues that the slow transport and moist air in China should lead to wet removal outside the Arctic.

Figure 4.16 shows the monthly variation in absolute contribution from China (dot-dashed line) and Europe (solid line) to the total zonal BC burden north of $60\,^{\circ}N$ in three different altitudes. Results from simulations with the original version are on the left and results with M7 on the right side. Figures 4.17 and 4.18 show the percentage contributions to zonal mean concentration with the original aerosol parameterization (top) and with M7 (bottom). Since the results from simulations with M7 are scaled by a factor five, all contributions are from a 100% of emissions of BC from fossil fuel sources. If M7 has a high degree of non-linearity, simply scaling the results will not necessarily equal contributions from an actual 100% reduction. To test the linearity in the system, two different regional experiments were conducted with M7, one where emissions were reduced by 20% and one with an 80% reduction. The results from the first reduction was scaled by a factor four to equal an 80% reduction, and the ratio of the contributions were then calculated. The result showed that the contributions from scaled results and actual reduction were similar in almost all regions, indicating a high degree of linearity. Therefore, the simple scaling of the results with M7 for comparison with the original aerosol parameterization should not lead to any large errors.

4.3.1 Original aerosol parameterization

First we look at the results from simulations with the original aerosol scheme. The largest contribution from China to the burden is found in the upper troposphere, as seen in Figure 4.16(e). There is seasonal pattern in the magnitude, seemingly following the change in vertical motions. The burden is highest in summer and early autumn, when convection is strongest. From October the burden is reduced from 0.15 $mg\ m^{-2}$ to less than 0.10 $mg\ m^{-2}$ in January, before starting a gradual increase again. This seems consistent with the theory in Stohl (2006) that emission from China

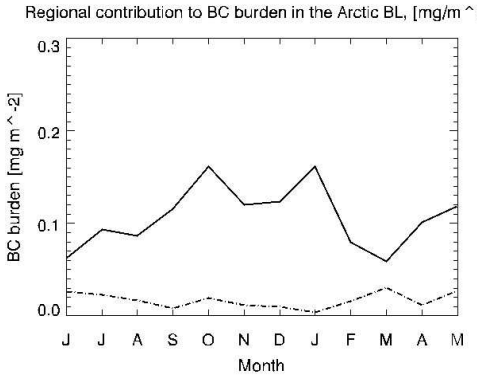

(a) Original

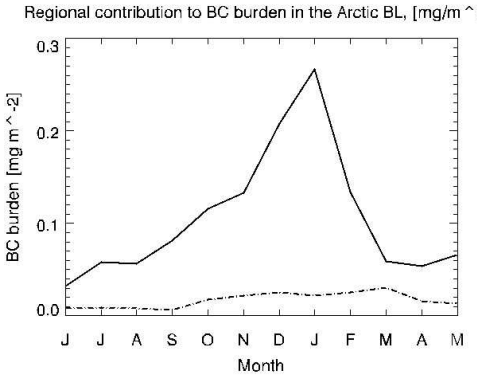

(b) M7

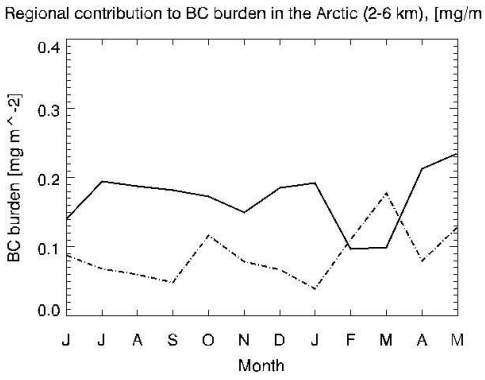

(c) Original

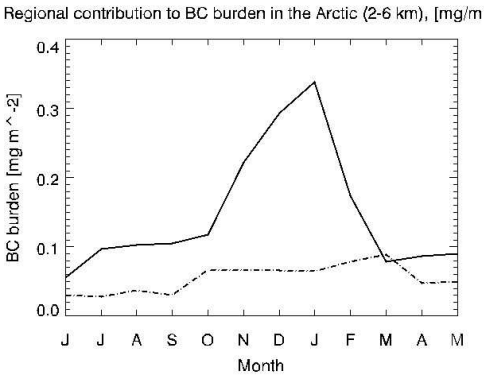

(d) M7

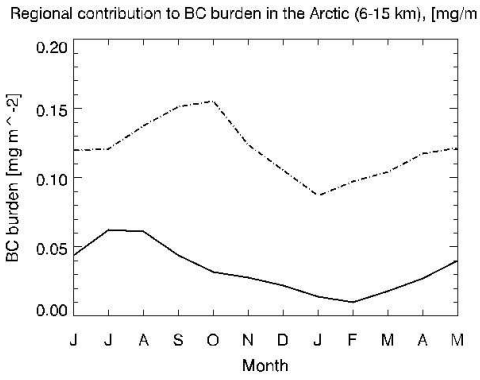

(e) Original

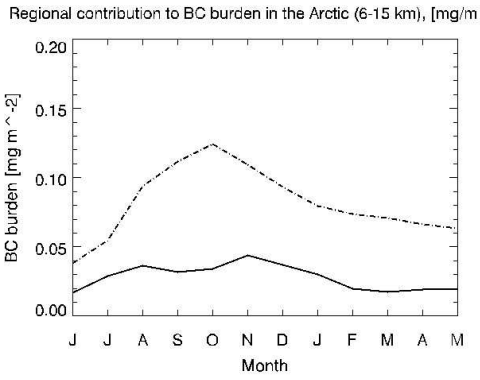

(f) M7

Figure 4.16: *Monthly contributions from fossil fuel BC from Europe (solid line) and China (dot-dashed line) to total zonal BC burden [mg m^{-2}] north of 60 °N in three different heights. Left panel shows simulations with the original parameterization and right panel with M7. Contributions between 0-1 km (top), 2-6 km (midldle) and 6-15 km (bottom).*

can follow a high altitude transport path to the Arctic. This pollution can potentially have an increased radiative forcing due to the underlying reflective surfaces, but downwards transport and following deposition in the Arctic snow and ice is almost impossible. Figure 4.17(b) shows the contribution to zonal mean concentration in July. Emissions in China contributes up to 50% to the high altitude BC concentration. The result also shows that China has siginificant contributions to the the BC transported to the Arctic in high levels. During winter, percentage contributions to zonal mean are reduced, especially in high altitudes. Figure 4.17(a) represents the typical fall and winter pattern, and values larger than $20 - 30\%$ are only found close to the source region. From Figure 4.16(a) it is clear that emissions from China has a minor impact on the burden in the lowest kilometer of the atmosphere in these latitudes. Throughout the whole year the burden remains less than $0.03\ mg\ m^{-2}$. A maximum in March is seen in Figure 4.16(a) and, more clearly, in Figure 4.16(c). This could be caused by the position of the Arctic front at that time. If it is located far south, then more of the pollution sources in Asia are behind the barrier and particles are more easily transported north, increasing the contribution. The monthly variation in the lower parts of the atmosphere displays less pattern than in the upper levels. With simulations for just one year, it is difficult to know how much of the monthly difference which is actually a pattern and how much is simply caused by the meteorological conditions that year.

While emissions from China dominate in the upper atmosphere, contributions from Europe are much larger below 6 km. This is seen clearly in both Figures 4.18 and 4.16. Figures 4.16(a) and (c) show that the burden from emissions in Europe is between 0.1 and 0.2 $mg\ m^{-2}$ below 6 km. Contribution in the lowest kilometer is largest from October to January, while there is less seasonal variation higher up, except for a strong decrease in February and March. Figure 4.18(a) shows that up to 70% of the total zonal mean BC concentration in the Arctic troposphere below 5 km is from Europe, but above 7 km the contributions are less than 20%. Again, the results are consistent with theory, showing the low-level transport northwards possible from sources in Europe. Percentage contributions from Europe are much smaller in summer, when emissions of BC from forest fires results in an increased contribution from other regions.

Annual mean contributions north of $60\,^{\circ}N$ from the CTM2 results (not shown here) are compared to the results in Koch and Hansen (2005) and Koch et al. (2007). The pattern in the CTM2 results agree well with their

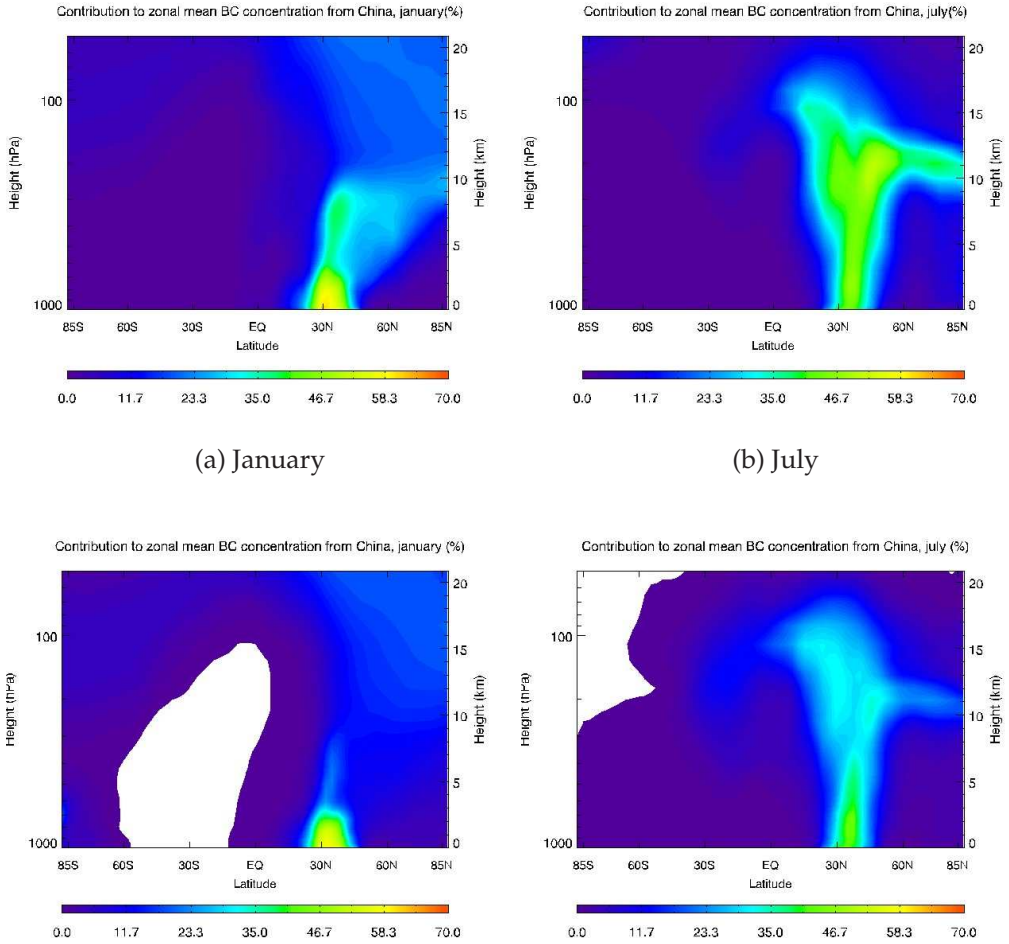

(a) January

(b) July

(c) January

(d) July

Figure 4.17: *Percentage contribution from fossil fuel BC from China to total zonal mean BC concentration with the original aerosol parameterization (top) and with M7 (bottom). White regions are small negative values, probably due to some degree of non-linearity in the M7 module.*

figures, but the magnitudes are slightly different. In Europe, the contributions below 5 *km* are approximately 10% larger with the CTM2, while low-level contributions from China are $5 - 10\%$ smaller. As mentioned, Koch and Hansen (2005) found contributions from south Asia in the upper troposphere and lower stratosphere of up to 50%, but they included India in this region. Koch et al. (2007) treated China as a separate region, as is done in this thesis, and found high-altitude contributions of $30 - 40\%$. This is

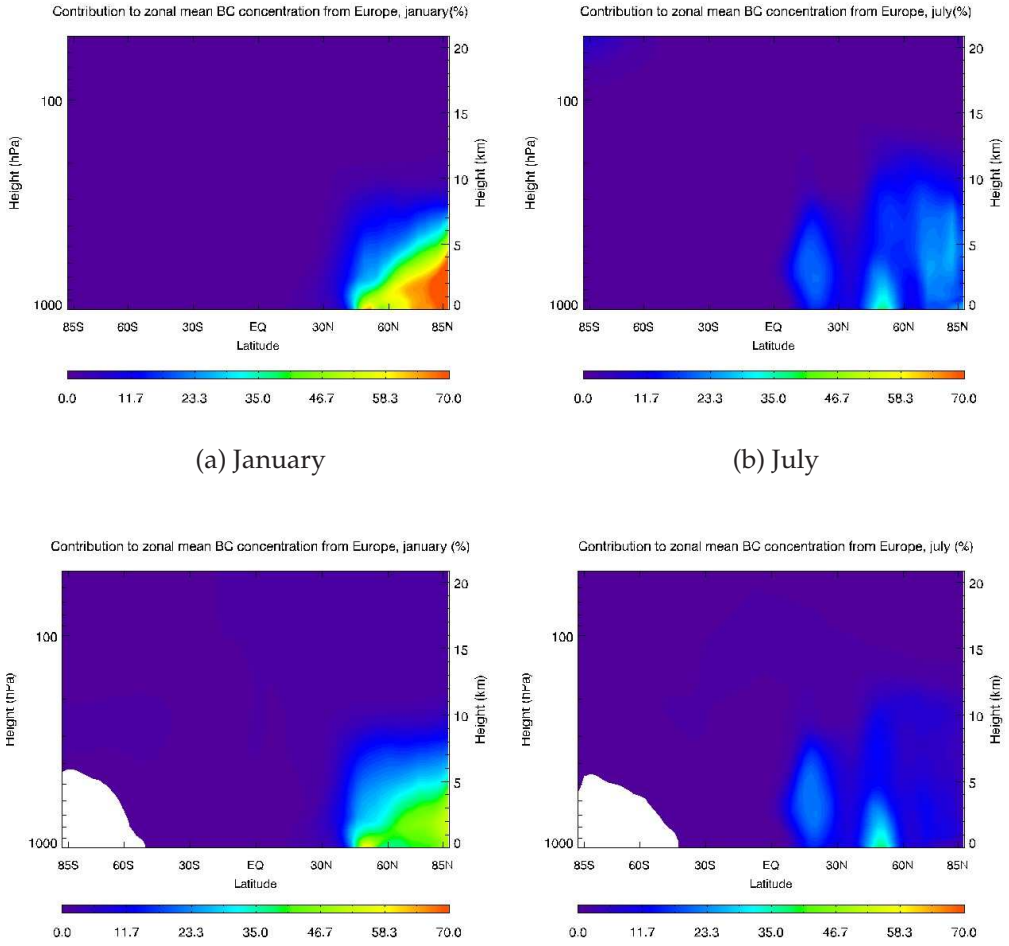

(a) January

(b) July

(c) January

(d) July

Figure 4.18: *Percentage contribution from fossil fuel BC from Europe to total zonal mean BC concentration with the original aerosol parameterization (top) and with M7 (bottom). White regions are small negative values, probably due to some degree of non-linearity in the M7 module.*

more in agreement with the CTM2 results, but still slightly higher. Results from the CMT2 model also agree well with results from a new study by Shindell et al. (2008), where European emissions are most important below 500 *hPa* and BC from China dominates higher up. The seasonal variation also agree well with results in this thesis. Their results are however weighted by emission in the different regions, so direct comparison with actual values is not possible.

4.3.2 M7

As expected, the choice of aerosol parameterization greatly influences the regional contributions. The right panel in Figure 4.16 show the regional contributions to the BC burden in the Arctic troposphere with M7. Emissions from China still dominate between 6 and 15 km, but values are smaller, especially in spring and summer. The burden is now only 0.04 $mg\ m^{-2}$ in July, compared to 0.12 $mg\ m^{-2}$ with the original aerosol representation. In lower levels, the burden from China is strongly reduced throughout the whole year, and there is much less monthly variation in the magnitude. This confirms that the BC aging is faster, leading to increased removal closer to the source. The shorter BC lifetime in China with M7 is also seen by comparing Figures 4.17(a) and (c), and 4.17(b) and (d) for the contributions to zonal mean concentration. Also here the difference is strongest in July and in high altitudes. BC from China contributes much less to the Arctic BC concentration when the regional difference in aging is accounted for. A faster aging in China is realistic, but as discussed in Section 4.2.1, the aging may be too fast. In such case, the contributions are underestimated as well.

Contributions from European emissions of fossil fuel BC with M7 confirm the strong seasonal variation in BC aging. During winter, the contribution to burden is strongly increased compared to the original results, while during summer the burden is smaller. When sunlight is absent, the aging is slower and wet removal is less efficient. More particles can therefore reach the Arctic atmosphere from Europe. During the summer the transfer is faster, resulting in a larger fraction removed outside the Arctic. The seasonal variation in contributions, with a maximum in winter and lower contributions in summer from Europe, is strenghtened with M7. This suggests that meteorological, dynamical and chemical processes are positively correlated. Stronger horizontal winds, less efficient wet removal and the extra transport path act together with slower aging in increasing the contribution to burden during winter. The absolute contributions to burden from Europe in lower levels are much larger than contributions from China, but Figures 4.18(a) and (c) reveals a strong decrease in percentage contribution during winter, despite the increased burden. BC from other source regions must therefore contribute more, and the aging time must be even slower than in Europe. BC sources in Russia and Eurasia are located in even higher latitudes than Europe, and the burden is expected to increase more. However, a full analysis requires more regional experiments.

Region	Aging time with original version [days]	Aging time with M7 [days]
China	4.16	3.16
Europe	4.16	5.16

Table 4.3: *Aging time in days for BC in Europe and China with the two aerosol parameterizations*

To summarize the results in this section, the contributions to BC in the Arctic lower troposphere are larger for Europe than for China, while in the upper atmosphere BC from China is more important. This is consistent with several other studies, and the pattern is further strenghtened with M7. The M7 module leads to a shorter BC aging time in China, and therefore a reduction in contributions. BC from Europe experience a seasonal variation in aging, with much slower transfer during winter and a shorter aging time during summer. To confirm the regional differences in aging, the aging time for both regions is calculated as

$$\tau_{aging} = \frac{Regional\ burden\ of\ soluble\ BC\ [Tg]}{Total\ emitted\ BC\ in\ the\ region\ [Tg\ yr^{-1}]}$$

Total emitted BC is 1.42 $Tg\ yr^{-1}$ and 0.42 $Tg\ yr^{-1}$ in China and Europe, respectively (Bond et al., 2006) [1]. Table 4.3 shows the results. A constant transfer of 24% equals a constant aging time of 4.16 days. With M7, annual mean aging time in Europe is 5.16 days, while the aging time for BC in China is reduced to 3.16 days. Seasonal differences are not evident here, but from the results above, aging time in Europe during winter is probably even more increased.

4.4 BC concentration in Arctic snow and ice

The reduced albedo of snow and ice due to absorbing impurities such as dust, volcanic ash and BC is not new knowledge. Of these species, the most effective contaminant is BC. One of the first to model snow albedo reduction was Warren and Wiscombe (1980). They also found that the effect of 1 $\mu g\ g^{-1}$ of soot was as large as the effect of 100 $\mu g\ g^{-1}$ of dust. Several studies of BC concentration and the effects on albedo has been made

[1] The region defined as Europe in this thesis covers slightly more than in Bond et al. (2006), while China is slightly smaller

since. Clarke and Noone (1985) collected snow samples in 1983-84 and found concentrations mostly in the range of $5 - 50\ ng\ g^{-1}$. More recent measurements have also been made. Grenfell and Light (2002) collected samples in the snow and ice in the Arctic Ocean during spring 1998. They found average concentrations of $4 - 5\ ng\ g^{-1}$. Measurements at ice-coring sites in Greeland showed values mostly below $4\ ng\ g^{-1}$ (McConnel et al. (2007), Slater et al. (2002)), with some occasional higher concentrations. Ice-cores can provide valuable information about historical concentration and sources of Arctic BC, and perhaps shed some light on the connection between BC and snow/ice reduction. These measurements are, however, made at only one location and may not be representative for the rest of the Arctic.

Reductions in BC emissions in Europe and the former USSR since the 1980s could mean the Arctic is cleaner now. Measurements of equivalent BC (EBC) at Alert and Barrow over 15 years do in fact reveal a strong decrease in concentrations during winter from 1990 to 2000 (Sharma et al., 2006). Reductions have also been stronger at Alert, which is more influenced by emissions from Europe and Russia. From 2001 to 2003, however, observations showed an increasing trend again. Throughout the 1990s the EBC content was higher at Alert, but towards the end of the period the concentrations are more similar at both stations. If the contributions from emissions in China are significant in Barrow, then the strong increase in BC emissions here may play a role in the observed increase. It is therefore important to know how different regions contribute to the BC concentration in the Arctic snow and ice

In the following sections, all maps of BC concentration in snow and ice are averaged over the top three snowlayers generated by the model and show monthly averages of March, April and May. These are calculated by summing the BC concentration each day and dividing by the number of days. This means that the daily variability in snow cover is not visible, and the monthly fields show BC in snow even if there was snow cover only for a few days during that period. This also means that radiative forcing calculations can not be done directly from this data as the result could be significantly overestimated. For this purpose, BC concentration has also been saved in 3-hour intervals.

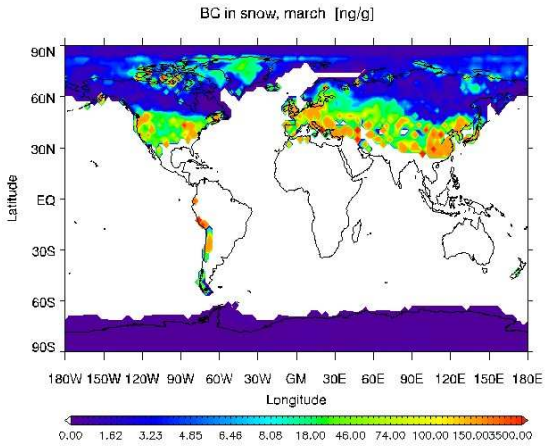

(a) March

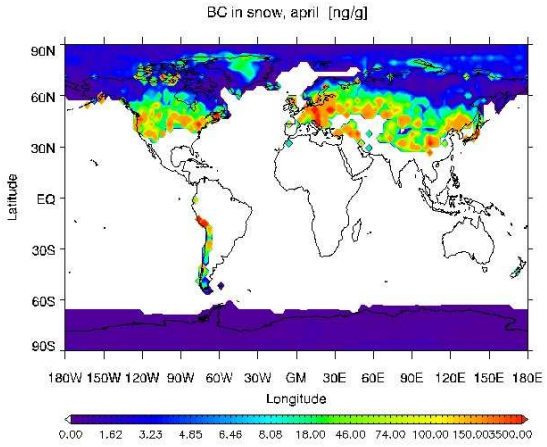

(b) April

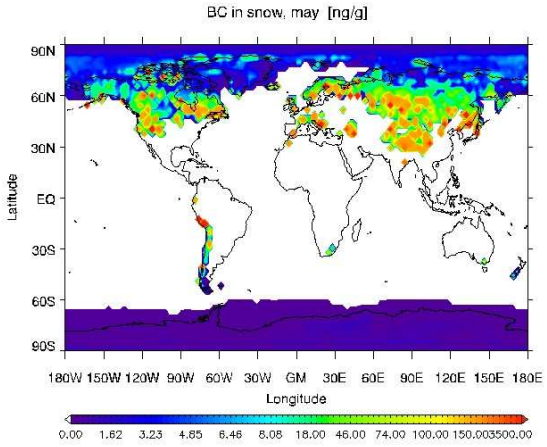

(c) May

Figure 4.19: *Concentration of BC from all sources in snow in (a) March, (b) April and (c) May with the original aerosol parameterization. Averaged over the top three model layers and in [ng* g^{-1}*].*

4.4.1 Original aerosol parameterization

Concentration

Figures 4.19 (a) to (c) show the distribution of the BC concentration in snow (in $ng\ g^{-1}$) for each of the three months. In the Antarctic, values are mostly less than 1 $ng\ g^{-1}$ and, as the main focus in this study is the Northern Hemisphere, no more attention is given to this area. In March, concentrations in excess of 150 $ng\ g^{-1}$ are found around China, in Europe and in some hot spots in Northern Canada and Central Asia. Maximum values reach more than 1 $\mu g\ g^{-1}$. In large parts of USA, Eastern Europe and Central Asia concentrations are between 20 and 70 $ng\ g^{-1}$. In Northern Asia and Canada, and in most of the ice and snow in the Arctic Ocean, concentrations are low, between approximately 2 and 8 $ng\ g^{-1}$. In April and May higher concentrations are found further and further north in Canada and Siberia due to accumulation of BC near the surface during melting. More of the hot spots with values higher than 1000 $ng\ g^{-1}$ also appear. Some of the highest concentrations are found in regions with boreal forest. Here, the radiative forcing and albedo reduction is less important as the snow cover is shielded from solar radiation by the trees. Maximum effect is expected on the Arctic tundra and sea ice and in the vast treeless areas in the North American Plains and in Central Asia in spring, and in the Arctic Ocean in summer (Warren et al., 2005).

Modeled concentrations from the CTM2 (Table A.5) are compared with modeled concentrations from Flanner et al. (2007) and measurements summarized in Table A.3. Both measurements and values calculated by Flanner et al. (2007) span large intervals, and the CTM2 results lie within the ranges at several locations, but always in the lower end. Measurements in the Arctic Ocean are from 1998 and match modeled values from the CTM2 well. CMT2 concentrations are also in the same range as the average values measured by Grenfell and Light (2002). In the French Alps, concentrations are much lower than the measurements. These samples are from 1992, and emission reductions in Europe may have lead to lower concentrations in the years after. Again, the coarse resolution in the CTM2 and the large BC variability complicates the comparison. The geographical distribution of annual mean concentrations of BC in snow from the CTM2 model (not shown here) agree well with Flanner et al. (2007), especially in mid-latitudes. In Northern Asia and Canada, and in much of the Arctic Ocean, the CTM2 concentrations are quite a bit lower. Some of

this difference can probably be explained by their use of biomass burning emissions from 1998. Annual emissions in 1998 was more than 1 Tg larger than in 2004, which is used here (Randerson et al., 2007). However, even when the biomass component is excluded in their results, modeled concentrations from the CTM2 (still including biomass burning BC) remain smaller in Canada and Siberia.

Climatic effects

Section 2.2 described several effects and feedbacks involved when BC is deposited in snow and ice. Here, some of these are revisited. Previous studies have estimated Northern Hemispheric albedo reductions due to BC in snow and ice of $1 - 3\%$ (Hansen and Nazarenko (2004), Jacobson (2004), Flanner et al. (2007)). However, as seen, the concentration of BC is not homogeneously distributed and the local albedo reductions can be higher close to source regions. When BC accumulates at the surface in spring and summer the climate effect is maximized because the timing coincides with increasing amount of incoming solar radiation at high latitudes and more coarse grained snow. This triggers further melting and more absorption of energy by the darker underlying surface. Figure 4.20 from Flanner et al. (2007) illustrates the albedo reduction with increasing BC concentration and also the strong dependence on snow grain size. Compared to the values without BC, hemispheric albedo is reduced by almost 0.05 for 100 $ng\ g^{-1}$ BC and with snow grain radius of 1000 μm, while the reduction for the same amounts of BC, but with snow grain radius of 150 μm is only 0.01. According to this figure, the albedo for old, melting snow can be reduced from 0.7 to 0.54 for the highest concentrations in from the CTM2 model (more than 1 $\mu g\ g^{-1}$). This equals 23%, and the reduction is significant also for more fine grained snow. Previous studies have shown that a BC concentration of 10 $ng\ g^{-1}$ is needed to cause an albedo reduction of 1% (Warren et al. (2005) and references therein).

Albedo reduction gives a positive radiative forcing, and can lead to changes in melt rate and near-surface temperature. Figures 4.21(a) and (b), which are also from Flanner et al. (2007), show calculated snow forcing from BC and change in snowmelt rate when BC is included in the snow and ice. Focusing on March, April and May, the maximum zonally averaged forcing is found around $55\,^{\circ}N$. The maximum moves north and strenghtens in April and May, reaching 1.5 Wm^{-2}. The melt rate increases during the beginning of the snowmelt season in high latitudes, and decreases in late

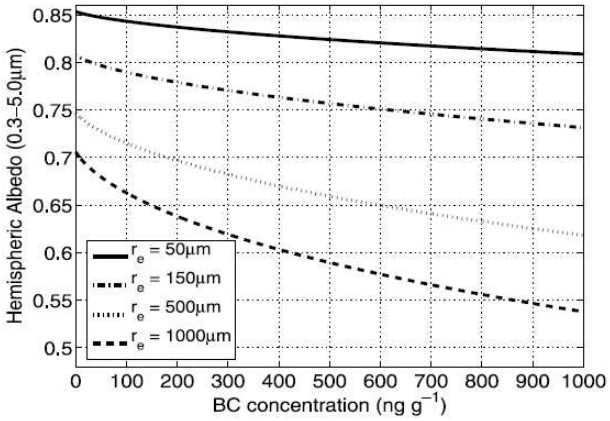

Figure 4.20: *Calculation of snow albedo as a functon of BC mass concentration for different snow effective radii from Flanner et al. (2007).*

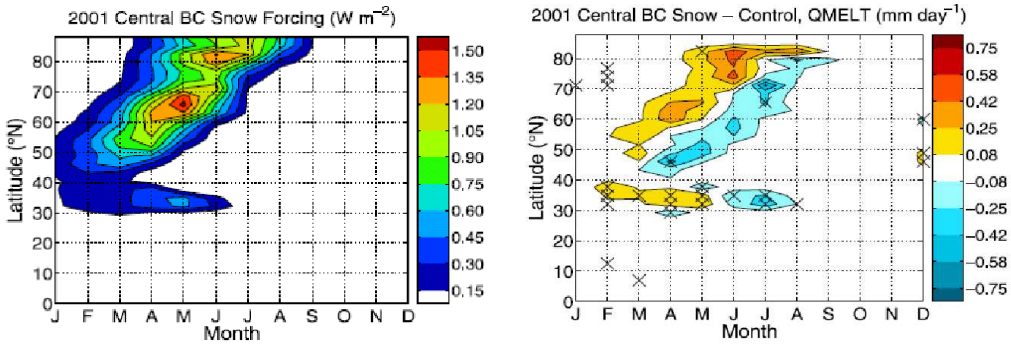

(a) Snow forcing

(b) Snowmelt rate

Figure 4.21: *Zonal monthly surface forcing from BC [W m^{-2}] (left) and difference in zonal monthly land snowmelt rate between experiment with BC and the control [mm day^{-1}] (right) (Flanner et al., 2007). Hatching shows statisically significant change at the 0.01 level.*

spring/early summer because there is less snow left. The energy which was previously used to melt snow can now warm the surface and atmosphere. Even though the albedo reductions may not seem very large, the climate impact can be strong due to the positive feedbacks involved.

Regional contributions

Now the attention is turned to the contribution to BC in snow and ice in the Arctic from the same regions. In section 4.3.1 it was seen that BC emitted in China is important in the upper troposphere and lower stratosphere, but that emissions in Europe dominate in lower levels. Theoretically, particles from Europe have the highest probability of deposition in the Arctic (Stohl, 2006). Furthermore, since downwards transport in the Arctic is slow, contributions from Europe are expected to be larger than in China.

Figure 4.23 shows the contribution of fossil fuel BC from Europe (solid line) and China (dot-dashed line) to the total BC content in snow and ice north of $60\,^{\circ}N$. This is a sum over all snowlayers and given in $mg\ m^{-2}$. It is important to keep in mind that this is the BC which has accumulated, not the actual deposition each month. The BC content is therefore highest in spring. When an entire snow column is melted, all BC in it is removed (Section 3.1.4) and the concentration during spring decreases. In the Northern Hemisphere, the snow in gridboxes with sea ice is assumed to melt at a constant rate from mid-April until June. On the 21st of June all snow in these areas is assumed to be gone (Skeie, 2007). This explaines sharp decrease in accumulated BC from June. The important feature here is that, as expected, the contribution from Europe is largest, despite the much higher emissions in China.

Figure 4.22 shows the percentage contribution from fossil fuel BC from Europe(left) and China (right) to the total BC in snow near the surface. European emissions contribute most to the BC concentration in the ice in the Arctic Ocean between $90\,^{\circ}W$ and $90\,^{\circ}E$, and there is a $10-30\%$ contribution in much of Russia and Central Asia as well. BC from China dominates between $150\,^{\circ}E$ and $150\,^{\circ}W$, with contributions between 30% and 60%. About 20% of BC in western North America comes from China, which is consistent with what Koch et al. (2007) found. BC emitted in China is not transported further west in Asia, as that would require transport against the dominating winds. Contributions from China in the Arctic Ocean between $90\,^{\circ}W$ and $90\,^{\circ}E$ are $10-20\%$, which is much smaller than

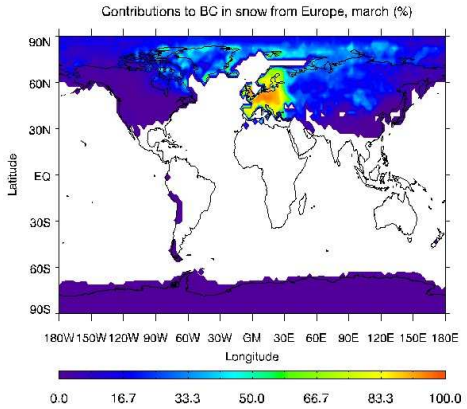

(a) Europe

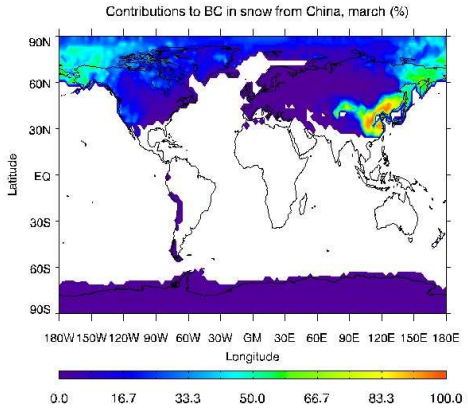

(b) China

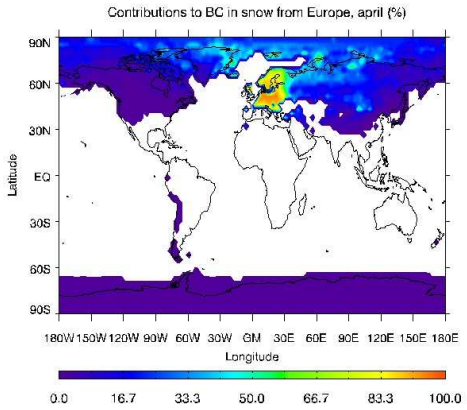

(c) Europe

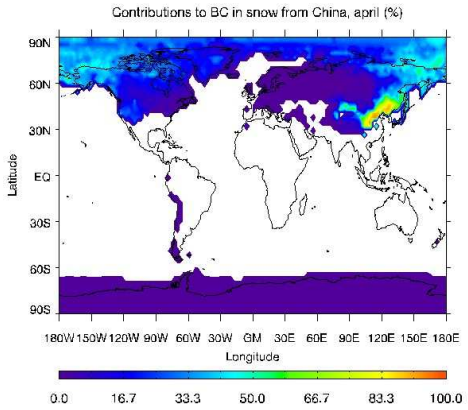

(d) China

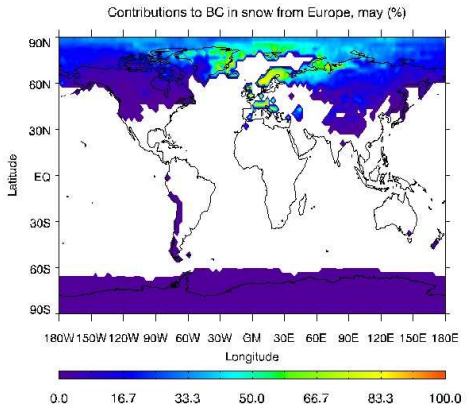

(e) Europe

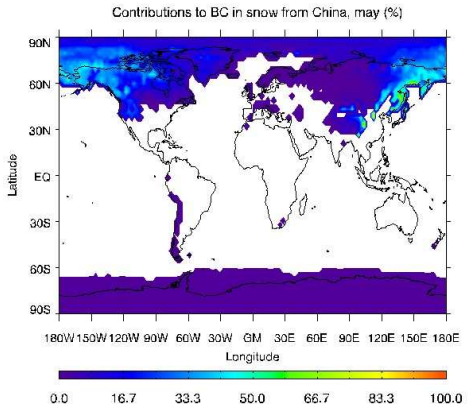

(f) China

Figure 4.22: *Percentage contributions from fossil fuel sources to the total BC concentration in snow. From Europe (left panel) and from China (right panel) with the original aerosol parameterization. For March (top), April (middle) and May (bottom).*

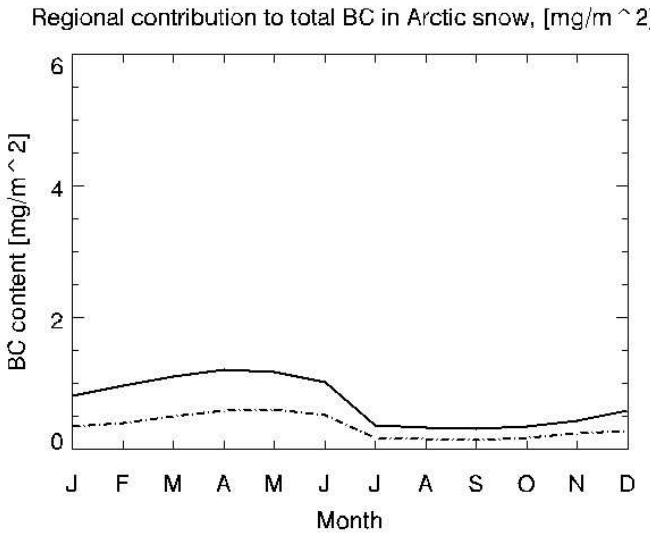

Figure 4.23: *Contributions from fossil fuel BC to total accumulated BC in snow north of* $60\,^{\circ}N$ *from Europe (solid line) and China (dot-dashed line) with the original aerosol representation. Sum over all layers and in unit* $mg\ m^{-2}$.

the European shares. There is a monthly variation in the contributions to BC concentration. The contribution from China is smaller in April and May than in March, while contributions from Europe are at a maximum in May. This is presumably due to variation in the position of the Arctic front, convective motions and precipitation. One quite interesting feature is that China does not appear to contribute significantly to the BC in the Himalayas, yet there has been reports of a decrease in glaciers (WWF Nepal Program, March 2005). The surface distribution also reveal high BC concentrations here. It would be interesting to do regional experiments with emissions from other areas to see where BC in this region originates from. In Canada, Central Asia and Siberia, where some of the highest BC concentrations are found (see Figure 4.19), the combined shares from China and Europe are less than half.

Other studies of regional impact have also found the largest contributions from Europe. Reddy and Boucher (2007) calculated contribution to surface deposition of BC north of $60\,^{\circ}N$, and found that Europe was the largest contributor (63%), followed by East Asia (17%). The contribution from East Asia is smaller than modeled here, but their source region covers all of south and southeast Asia, including Indonesia, as well as Mongolia and

large parts of Eurasia. Shindell et al. (2008) found the largest contribution to deposition in the Arctic (excluding Greenland) from Europe.

4.4.2 M7

Section 4.2.1 showed that changing the aerosol parameterization results in larger near-surface concentrations in the Arctic. Nevertheless, Figure 4.24 shows lower concentrations of BC in snow and ice north of the polar circle with the M7 module than in the original simulations. This is due to the fact that most of the BC transported here in winter is in the insoluble Aitken mode and can not be removed by precipitation, which was seen by comparing 4.11 and 4.13 in high latitudes. As shown in Section 4.1.3, dry deposition gives only a minor contribution to the total loss of BC particles, and hence concentrations are reduced. As an example, compare modeled near-surface concentration and concentration in snow and ice in Spitzbergen (Tables A.4 and A.5) with the two aerosol parameterizations. Near-surface concentration with the original version and with M7 is 8 $ng\ m^{-3}$ and 20 $ng\ m^{-3}$, respectively. The BC concentration in snow and ice, however, decreases from 6.7 $ng\ g^{-1}$ with the original version to 1.7 $ng\ g^{-1}$ with M7. In addition, the shorter aging time for BC in China reduces transport to the Arctic. Concentrations between 30 $^{\circ}N$ and 60 $^{\circ}N$ remain large. The discrepancy between the annual mean concentrations modeled in Canada, Siberia and the Arctic Ocean by Flanner et al. (2007) and by the CTM2 model is even larger with M7. Concentrations are also lower than most of the measurements in Table A.3.

Again, applying the M7 aerosol representation leads to changes in the regional contributions, as shown in Figures 4.26 and 4.25 for contributions to accumulated BC and percentage contributions to BC concentration near the surface, respectively. The European contribution to accumulated BC increases dramatically, from a maximum of 1.0 $mg\ m^{-2}$ with the original parameterization to almost 6.0 $mg\ m^{-2}$ with M7. Section 4.3.1 showed a slower BC aging in Europe and an increased contribution to the atmospheric burden. More BC particles can therefore reach the Arctic atmosphere than in the original simulation. However, more particles are also deposited in the region, showing that the lifetime is still not long enough for transport through the Arctic. Consistent with the shorter aging time, the contribution from China to accumulated BC in snow and ice strongly decreases, and is now negligible compared to the European influence.

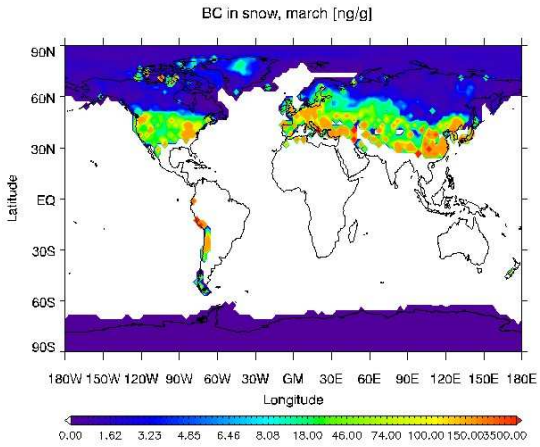

(a) March

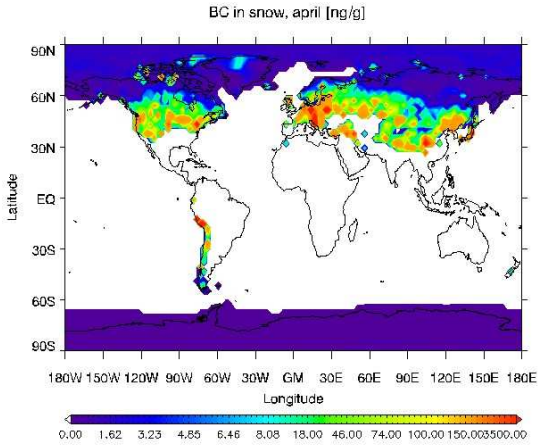

(b) April

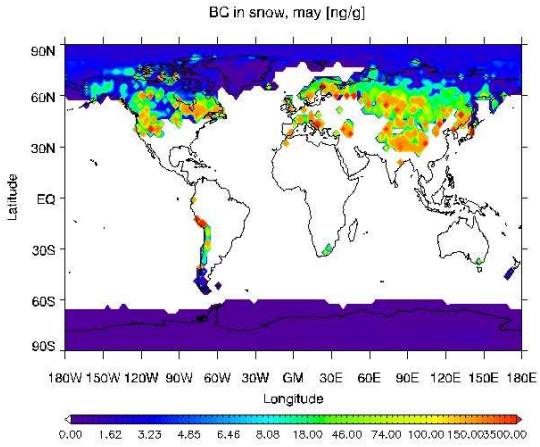

(c) May

Figure 4.24: *Concentration of BC from all sources in snow in (a) March, (b) April and (c) May with M7. Averaged over the top three model layers and in unit [ng* g^{-1}*].*

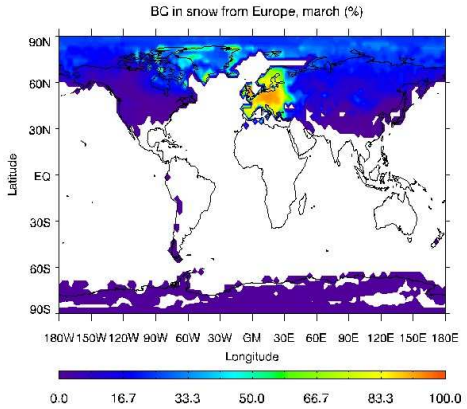

(a) Europe

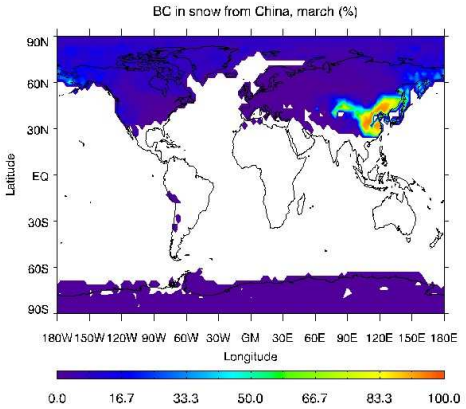

(b) China

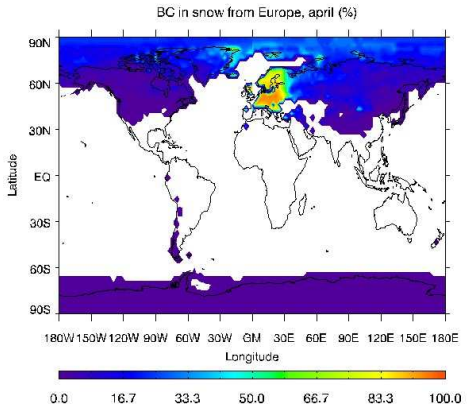

(c) Europe

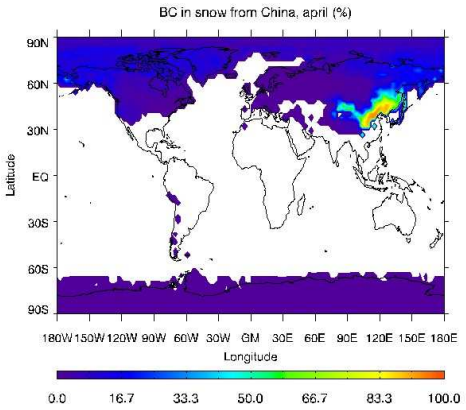

(d) China

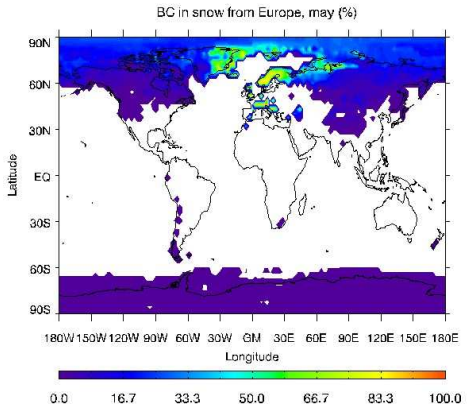

(e) Europe

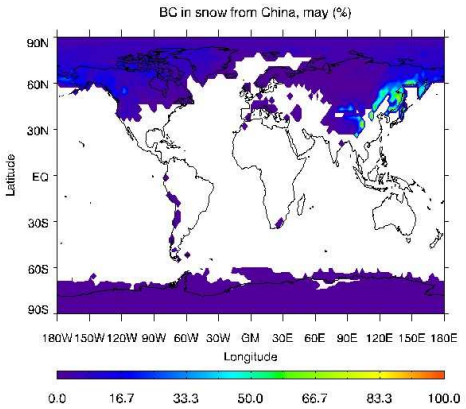

(f) China

Figure 4.25: *Percentage contributions of BC from fossil fuel sources to the total BC concentration in snow. Emissions from Europe (left panel) and from China (right panel) with M7. For March (top), April (middle) and May (bottom).*

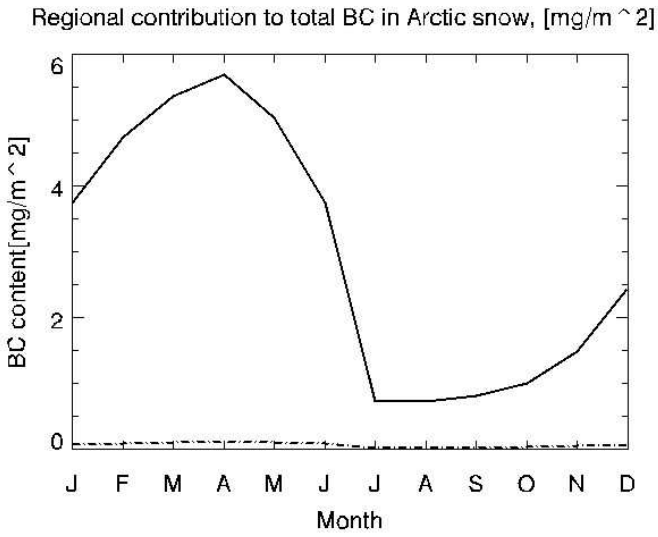

Figure 4.26: *Contributions from fossil fuel BC to total accumulated BC in snow between* $60\,^{\circ}N$ *and* $90\,^{\circ}N$ *from Europe (solid line) and China (dot-dashed line) with M7. Sum over all layers and in unit* $mg\ m^{-2}$.

Even though concentrations of BC in snow and ice are smaller in the Arctic, the absorption may be stronger due to the reflecting material in the mixed particle.

Percentage contributions show little change compared to the original version for European emissions. A slightly stronger contribution between $150\,^{\circ}E$ and $150\,^{\circ}W$ can be seen, while a very small decrease in contribution is seen over Russia. For emissions from China, the effect is larger. From providing a contribution of up to 50% in some regions, emissions from China now stand for only $10 - 15\%$ of the total BC in those same areas. In the rest of the Arctic Ocean contributions from China are mostly less than 10%. The only large contributions from China is found close to the source. Annual mean BC concentrations (not shown here) also reveal a decreased BC concentration in regions where emissions from China were important in the original version (Alaska, northeast Asia).

Summary

The results in Section 4.4 have shown that the concentration of BC modeled by the CTM2 compare reasonably well with measurements, though in the lower intervall. There is high variability in the concentrations, ranging from less than 10 $ng\ g^{-1}$ in the snow and ice in the Arctic Ocean, to more than 1 $\mu g\ g^{-1}$ near industrialized areas. From the albedo changes and forcings estimated in Flanner et al. (2007), the effects of the concentrations modeled in this thesis with both aerosol parameterizations can be significant. As expected from previous experiments and theory, emission of fossil fuel BC in Europe has a larger impact on the BC concentration in the Arctic than emissions in China. Maximum percentage contributions to BC in snow and ice from China and Europe are of relatively equal magnitude, but only in limited areas. Europe dominate in a larger part of the Arctic Ocean, and emissions are also transported into Central Asia and Russia.

Accounting for regional differences in aging changes the regional contributions. The increased aging time for BC emissions in Europe strengthens the contribution to accumulated BC, while contributions from China become negligible. The near surface concentration is, however, lower in the snow and ice in the Arctic Ocean. This is due to the shorter aging time in China, and to an even slower aging in Russia and Eurasia than in Europe, which means more BC from this region remains insoluble. More measurements to compare modeled concentrations to are necessary in order to better evaluate how accurate the regional BC aging in M7 is.

4.4.3 Effect of increased SO_2 emissions

Emissions consist of a mixture of many different gases and particles, and reducing or increasing one species will affect the others. This is important because emission reductions can have unforeseen consequences. The particle interaction in M7 allows us to study how reduction in one or more species affect the lifetime and concentration of co-emitted components. In this experiment SO_2 emissions from the industry and power plant sector in Europe was increased by 70%. This allows for a further investigation of the BC/ sulphuric acid relationship which is so important for aging in M7. As described in the introduction, higher emissions of SO_2 should give a faster aging of BC, and a lower concentration in snow and ice is expected. This belief is further strengthened from the results for BC in China. Comparison of the results from this test and the control run with original

emissions was done for BC burden, zonal mean concentration and deposition on snow and ice.

The percentage change in annual mean burden, calculated as the ratio of burden with changed emissions to the control, is displayed in Figure 4.27(a). The annual BC burden is up to 10% smaller with higher SO_2 emissions. The change occurs north of 60 $^\circ N$ and the largest difference is found between 30 $^\circ E$ and 90 $^\circ E$, but there are also smaller changes in much of the rest of the Arctic. This shows that a local change can have widespread effect. The decreased atmospheric concentration is also seen in Figure 4.27(b), which shows the ratio of annual zonal mean concentration with increased emissions to the control simulation. Again, there is negligible effect in all latitudes except north of 60 $^\circ N$. The same changes, but in January and July, were also investigated. The results show a negligible effect on burden in July, while the impact from more SO_2 is maximized in winter. Figure 4.27(c) shows percentage change in BC concentration in snow and ice in March. With higher SO_2 emissions, more BC is deposited in the Arctic and the concentration is increased by up to 10% over a large area.

As expected, higher SO_2 emissions did reduce the aging time for BC, which is seen from the lower atmospheric BC concentration. Because production of sulphuric acid is more efficient during summer, the largest difference was expected to occur in this season. That the difference was largest during winter, and that the largest reduction in atmospheric concentration happened some distance away from the sources, was therefore surprising. The expected reduction in BC concentration in the Arctic snow and ice did not occur. The explanation lies in the relationship between aging time and depostition. Figure 4.28 gives a simple illustration. Slower aging means that the lifetime is longer. It appears that up to a certain point, increasing aging time leads to more deposition in the Arctic. More particles reach this area, but the lifetime is still short enough for removal here. After that, further increase in aging time results in a lifetime which is too long, and more particles are transported through the region.

The vertical dashed lines illustrate how BC aging in Europe varies. Using M7 leads to a strong increase in aging time during winter compared to using constant transfer, which was seen by the increased burden in Figures 4.16(b) and (d). Because of this, more BC particles reach the Arctic, and the aging time is still short to increase deposition compared to the original version. Higher SO_2 emissions move the BC aging time towards lower

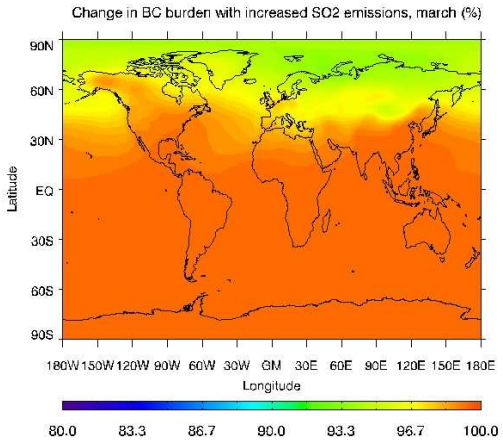

(a) Annual burden

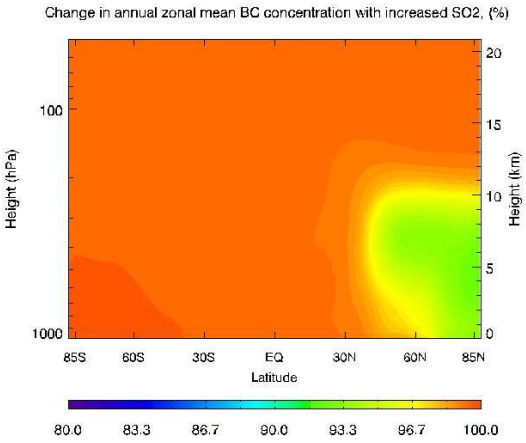

(b) Annual zonal mean

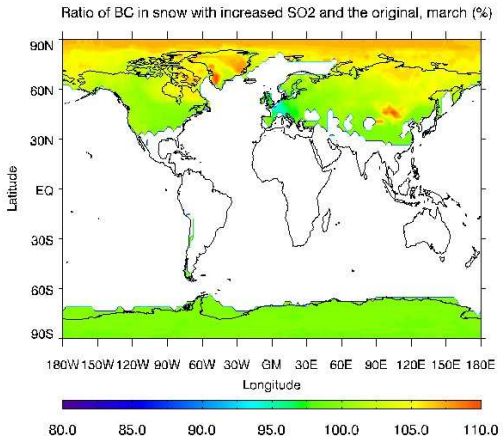

(c) BC concentration in snow

Figure 4.27: *The effect of* 70% *higher emissions of* SO_2 *from the industry and power plant sectors in Europe (in per cent) with M7. BC burden (top), zonal mean concentration (middle) and concentration of BC in snow and ice (bottom).*

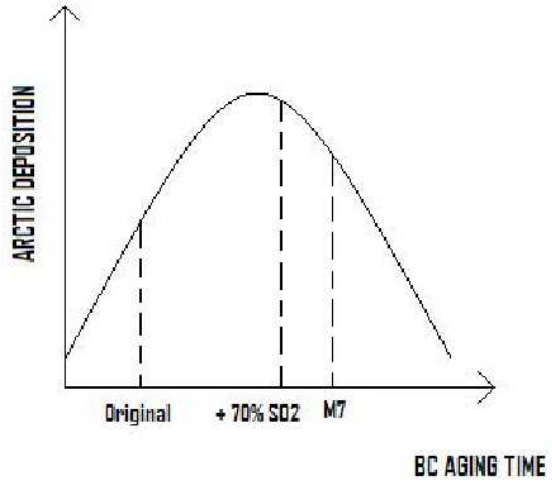

Figure 4.28: *The relationship between aging time and deposition in the Arctic. Deposition increases for increasing aging time up to a certain point, when the aging becomes so slow that more is transported through the Arctic region. Vertical lines illustrate how the aging for BC emitted in Europe varies with the original parameterization, with M7, and with increased SO_2 emission.*

values again, but at the same time increasing deposition in the Arctic. In summer, the effect is less important because the aging time is shorter and the particles are already removed efficiently.

Assuming that M7 accurately represents BC aging in Europe, increased SO_2 emissions lead to more BC in the snow and ice in the Arctic Ocean. This is not necessarily true for similar increases in other regions. Transport time for BC from China to the Arctic is most likely longer, and increasing SO_2 could remove the particles fast enough to reduce deposition in the Arctic. Also, if M7 overestimates the aging time during winter in Europe, it is not evident that increased SO_2 emissions will increase the amount of BC in Arctic snow and ice.

In this experiment SO_2 emissions were increased while emissions of BC remained unchanged. The two aerosol species are co-emitted, especially in the industry and power sector (Koch et al., 2007), and BC emissions were also much larger in Europe earlier. The effect of more SO_2 could be different if BC is also increased. This is however not tested here.

4.5 Mitigation

Even though BC and other aerosol species are known to have important climate effects they are not included in any global climate agreements today. There are many arguments both pro and con including these species, and there has been many discussions on the subject, such as Rypdal et al. (2005), Bond (2007), Hansen et al. (2000). One issue is finding ways to measure and compare the climate effects of the spatially heterogeneous and short-lived aerosol species with the well-mixed long-lived greenhouse gases (LLGHG). A common metric is global warming potential (GWP). The GWP is the radiative forcing from a pulse emission of an atmospheric species integrated over a chosen time horizon relative to the radiative forcing from the same emission of CO_2. Rypdal et al. (2005) discuss several problems with this concept. Originally, GWP only considers global effects. Several of the climate effects from BC and other aerosols may be mainly regional. The GWP has to be calculated depending on the emission region and the effect in question. Calculations of GWP for BC was made in Reddy and Boucher (2007) and Bond and Sun (2005), and results show that there are large uncertainties in the estimates. Berntsen et al. (2006) used a related metric called Warming Index (WI) and found strong regional differences. Reddy and Boucher (2007) also made preliminary calculation of GWP for the snow albedo effect of BC. Additionally, GWP also strongly depends on the chosen time horizon and comparing components with very different lifetimes is not straightforeward. Short-lived species will be given more weight when evaluated over a short time horizon, than over a 100 year period. For example, the lowest estimate of $GWP_{BC,100}$ was found to be 210, while $GWP_{BC,20}$ was 690 (Bond and Sun, 2005).

BC is a primary aerosol species, i.e. it is emitted directly, and must be regulated at the source. The technology to reduce emission is already available, but mitigations also have to be cost effective and politically attractive. Bond and Sun (2005) suggests that most reduction efforts are either too expensive or to difficult to enact compared to LLGHGs in most industrialized countries, but can be important for nations that have not agreed to adress LLGHG emissions. The attractiveness of reducing aerosols can be increased by co-benefits in terms of health and air quality.

This thesis has shown that BC emissions in Europe have a larger impact in the Arctic than BC from China, and in this aspect, reducing BC in Europe is important. The results from the regional experiments also reveal that in

many areas with high BC concentration, for example in the Himalayas and central Asia, neither China nor Europe contributes most. Reduction efforts need to be considered for other regions as well. BC emissions in China are, however, large and growing. The Arctic contribution from China was strongly affected by the choice of aerosol parameterization, reflecting uncertainties in the regional impact. Furthermore, reductions in Asia may be more effective from an economic perspective, and will lead to large improvements in air quality and health. Reduction efforts in China should therefore not be excluded based on the importance in the Arctic.

Mitigations aimed at reducing BC will affect the co-emitted species, including the scattering particles which today mask the warming. The net effect of reducing BC is therefore uncertain. Either way, reducing BC particles will only give a short term, temporary reduction to global warming, and it is important to keep focus on the LLGHG.

Chapter 5

Conclusion

5.1 Summary and conclusion

The chemical transport model Oslo CTM2 has been used to study the effect of two different parameterizations for BC aging on the lifetime, concentration and transport. In the original parameterization aging is determined by a constant transfer of 24% per day from hydrophobic to hydrophilic mode, which means the aging time is equal for particles in all regions. This is of course not a physically correct representation, although the rate can be adjusted to achieve good agreement with observed BC concentrations. In reality, BC becomes hydrophilic through condensation by gas-phase sulphuric acid, coagulation and/or through oxidation. The aging time will therefore vary in different regions, depending on the amount of SO_2 emitted and the oxidation capacity of the atmosphere. A new microphysical aerosol parameterization includes particle interaction, and also describes size distribution and mixing state of aerosols. Several model simulations was conducted to test the M7, and here the main features are summarized.

Concentrations of BC are highest close to source regions, reaching several $\mu g\ m^{-3}$ in the lowest surface layer. BC has a short lifetime and is removed relatively close to the sources, mainly by large-scale wet removal. Both vertical and horizontal distribution of concentration reveal the rapid derease away from source regions. The distributions further reveal that regional and seasonal differences in dynamical and meteorological conditions affect lifetime and concentration of BC. With the original parameter-

ization, global annual burden and lifetime is 0.17 Tg and 7.63 days, and the aging time is 4.16 days.

Including particle interaction, leads to regional and seasonal differences in aging. Chemistry now acts together with dynamics and meteorology in determining lifetime. In high latitudes, aging is slower during winter than in the original parameterization. Less BC is removed and near-surface concentrations increase. In lower latitudes, the aging is faster and concentrations are reduced more rapidly. Global annual burden and lifetime for BC is only slightly changed with M7, to 0.14 Tg and 7.3 days.

CTM2 calculations of the amount of BC in snow and ice in the Northern Hemisphere show high concentrations near industrialized areas and on the continents, especially when BC accumulates during melting. BC content in ice and snow in the Arctic Ocean is less than 10 $ng\ g^{-1}$ during spring. Based on previous calculations, the climate effect of the concentrations found in this thesis may be significant.

Regional experiments reveal that Europe contributes more to the BC burden in the Arctic lower troposphere, while the contribution from China is larger in the upper troposphere. As expected based on theory, European emissions also contribute more to the accumulated BC in the Arctic snow and ice. This result is in agreement with several other studies, though the magnitude of contributions differ somewhat. The result seem quite robust, as it is confirmed when M7 is applied.

Regional experiments with M7 confirm the variation in aging time. Aging for BC in China is faster than originally, especially in summer. More BC is removed outside the Arctic, reducing contributions to BC burden and accumulated BC in snow and ice. Annual mean aging time in China is reduced to 3.16 days. Aging for BC emitted in Europe show a strong seasonal variation. Aging during winter is much slower due to lower production of sulphuric acid when sunlight is absent, and more BC can reach the Arctic and be deposited there. Contribution to BC burden and accumulated BC in snow and ice is therefore strongly increased. During summer, aging is faster than in the original parameterization. Annual mean aging time is increased to 5.16 days. When accounting for regional differences in aging, contributions from China in the Arctic become negligible compared to the European impact. This is presumably due to a combination of higher SO_2 emissions and less seasonal variation in incoming solar radiation in China. M7 seems to strengthen existing monthly trends.

To study the relationship between BC and sulphuric acid, emissions of SO_2 was increased by 70% in Europe. This resulted in up to 10% more BC deposited in the Arctic, not less as expected. The aging is faster, but the transport time is short enough that particles still reach the Arctic. More particles are deposited there instead of being transported through. This is not a general conclusion, however, since the effect may be very different for BC in other regions where transport time is longer.

Concentrations of BC from the CTM2 model are generally lower than observations and measurements. There are some indications that the aging in M7 may be too fast in lower latitudes. However, this can not be concluded with certainty at this time due to few observations and measurements, the coarse resolution in the CTM2 model and the high variability of BC in time and space. There is also a lack of observations in high latitudes to compare the increased near-surface concentration with M7 to.

Aging is a key parameter in determining the lifetime of BC. This thesis has shown that using M7 leads to regional and seasonal variations in BC aging, and the results are consistent with changes in atmospheric concentrations and deposition. The main results are also as expected based on theory. More work is needed to evaluate how accurate the aging in M7 is, and there is room for improvement. The inclusion of this module is still an important step towards improved aerosol modeling, since the most important argument for using M7 is that microphysical processes can be studied. Particle interaction is important because it leads to the formation of internally mixed particles, which has consequences for optical properties and removal processes. M7 may improve calculation of radiative forcing, and regional impact can be determined more accurately. Furthermore, M7 allows us to study the effect of simultaneous changes in emissions of several pollutants, such as O_x (OH, O_3, H_2O_2), SO_2, and BC, and the effect of mitigations depending on location. This is important for the developement of new technology and scenarios for future emission reductions, and for the calculation of GWP.

5.2 Further work

One major challenge concerning BC is the emission inventories. Emissions are based on energy consumption and emission factors for the dif-

ferent fuels, both of which are uncertain. Improved emission data and more observations of BC in the atmosphere would help in the evaluation of the model performance with the two aerosol parameterizations. More measurements of BC in Arctic snow and ice are under way as part of the International Polar Year, and hopefully it is possible to compare model results with these at a later time. Further work with this subject also has to include more regional experiments, since those that were conducted in this thesis are insufficient to give a full analysis. This work has already been started. In this thesis only the regional contribution to accumulated BC was investigated. New model simulations should also include an output of the actual deposition. Calculations of radiative forcing of BC in snow and ice with both parameterizations can reveal the effect of having internally mixed particles in the snow pack. There are some indications that M7 underestimates BC concentration in low latitudes. In such case, the condensation and coagulation schemes need to be further tested and potentially improved.

Appendix A

Observed and modeled concentrations

The following tables from Jacobson (2002) and Flanner et al. (2007) contain measurements and previously modeled concentrations of BC close to the surface and in snow. Values from the highlighted stations are compared to the results in this thesis. Results from the CTM2 model at the same stations and period are summarized in the last two tables.

Table 1. Comparison of Modeled Versus Observed Near-Surface BC Concentrations

Station	Latitude	Longitude	Modeled BC (ng/m^3)	Measured BC (ng/m^3)	Period	Data reference
			Marine			
Amsterdam Island	37°30′S	77°10′E	8.5	5.5	Annual	*Cachier et al.* [1994]
Atlantic Ocean	31–37°N	66–76°W	160	10	January–February	*Quinn et al.* [2001]
	15–31°N	43–66°W	45	10		
	8–15°N	33–43°W	65	30		
	3–8°N	26–33°W	220	360		
	5°S–3°N	17–26°W	180	380 ± 210		
	25–5°S	6°E–17°W	50	20 ± 30		
	33–24°S	18–6°E	90	10		
Bermuda	32°45′N	65°W	70	30	February	*Wolff et al.* [1986]
			80	40	August	
Böisto Island	60°20′N	26°30′E	1030	50–1000	June	*Raunemaa et al.* [1993]
Chichi-jima	27°N	142°E	175	610	December	*Ohta and Okita* [1984]
Corsica	42°N	9°E	420	380	Spring	*Cachier et al.* [1989]
East China Sea	27–32°N	127–129°E	370	355	April–May	*Parungo et al.* [1994]
	27–33°N	124–129°E	810	505	October–November	
	28–32°N	125–128°E	920	133	December	
Hachi-jima	33°5′N	139°45′E	885	1070	January	*Ohta and Okita* [1984]
			845	740	December	
Halley Bay	75°24′S	27°W	2.7	0.3–3		*Cachier et al.* [1986], *Hansen et al.* [1988]
La Réunion Island	21°30′S	55°30′E	70	50–650	Annual	*Bhugwant et al.* [2000]
Mace Head, Ireland	53°20′N	9°54′W	490	26 (17–34)	July–August	*Krivacsy et al.* [2001]
			450	47–1041	Annual	*Derwent et al.* [2001]
NE Atlantic			80	268	October–November	*O'Dowd et al.* [1993]
NE Pacific	27–48°N	175°E	60	150–300	April–October	*Kaneyasu and Murayami* [2000]
Ny-Alesund	78°54′N	11°53′E	150	70 (28–174)	March–May	*Heintzenberg* [1982]
			170	293 (123–567)	March–April	*Clarke* [1989]
Oki Island	36°9′N	133°12′W	55	520	Annual	*Mukai et al.* [1990]
San Nicolas Island	33°9′N	119°18′W	240	260	Annual	*Kim et al.* [2000]
			Rural			
Abastumani	41°30′N	42°40′E	460	980	Annual	*Dzubay et al.* [1984]
Abisko	68°18′N	18°30′E	300	393	March–April	*Noone and Clarke* [1988]
			360	259–780	Annual	*Clarke* [1989]
Allegheny	40°N	79°W	820	1300	August	*Keeler et al.* [1990]
Aspvreten, Sweden	58°48′N	17°23′W	115	100 (50–170)	June–July	*Zappoli et al.* [1999]
Cheboque Point	43°48′N	66°6′W	270	81–139	August–September	*Chylek et al.* [1996]
East Arctic	79°33′N	90°37′E	125	25–115	March–April	*Polissar* [1993]
Ecuador	2°S	77.18°W	265	100–520	Annual	*Andreae et al.* [1984]
	2°15′S	79°52′W	430	100–520	June	
Florida	28°N	82°W	690	400	Annual	*Andreae et al.* [1984]
Gif sur Yvette	48°42′N	2°8′E	1300	1650–2750	Seasonal	*Cachier et al.* [1989]; *Brémond et al.* [1989]
Jungfraujoch, Switzerland	46°33′N	7°59′E	710	290 (8–720)	July–August	*Krivacsy et al.* [2001]
K-Puszta, Hungary	46°57′N	19°42′E	1670	810	Annual	*Heintzenberg and Mészáros* [1985]
			1700	600 (400–600)	July–August	*Zappoli et al.* [1999]
			1700	750 (120–1890)	July–August	*Krivacsy et al.* [2001]
Landes forest	44°N	1°W	350	300	Autumn	*Cachier et al.* [1989]
Lin'an	30°15′N	119°42′E	2150	2070	July–August	*Parungo et al.* [1994]
North Carolina	35°18′N	80°W	550	520	Annual	*Andreae et al.* [1984]
Nylsvley, South Africa	24°39′N	28°24′E	340	850 (450–1340)	May	*Puxbaum et al.* [2000]
Petten	52°54′N	2°55′E	1360	1630	April	*Berner et al.* [1996]
Rorvik	57°18′N	12°12′E	1010	725	January–May	*Broström-Lundén et al.* [1994]
Senonche	48°34′N	12°E	1100	1200	March	*Cachier et al.* [1990]
Southwest United States	34°18′N	106°W	160	150–220	Annual	*Andreae et al.* [1984]
West Mountain	40°N	116°E	720	1710–2610	August	*Parungo et al.* [1994]
Maldives	4°58′N	73°28′E	290	2700–9400	February	*Chowdhury et al.* [2001]
			Urban			
Arnhem	52°N	5°54′E	1600	2950	October–November	*Janssen et al.* [1997]
Atlanta, Ga.	33°N	85°W	460	1500 (500–3000)	August	*Modey et al.* [2001]
Baltimore			800	530–2600	July	*Brunciak et al.* [2001]
Beijing	40°N	116°E	680	8700–10,100	Annual	*He et al.* [2001]
			700	6270	Summer	
			640	10,230	Autumn	
			690	11,080	Winter	
			680	6670	Spring	
Chicago/Lake Michigan	41°31′N	87°39′W	970	340–420	January	*Offenberg and Baker* [2000]
			1050	350–490	July	
Chesapeake Bay	38°40′N	76°25′W	790	400–7300	July	*Brunciak et al.* [2001]
Clermont Ferrand	45°46′N	34°E	1270	2400	April	*Lyubovtseva and Yatskovich* [1989]

Figure A.1: *Observed and modeled BC concentrations from Jacobson (2002).*

Table 1. (continued)

Station	Latitude	Longitude	Modeled BC (ng/m^3)	Measured BC (ng/m^3)	Period	Data reference
Dushanbe	38°33′N	68°48′E	290	10,700–12,000	August–September	*Hansen et al.* [1993]
Gorlitz	51°10′N	14°59′E	1950	1300	Annual	*Zier* [1991]
Halle	51°29′N	12°E	1800	1600	Annual	*Zier* [1991]
Hamburg	53°52′N	9°59′E	2800	1975	Annual	*Heintzenberg and Mészáros* [1985]
Kaohsiung			1400	3300–8000	November–April	*Lin and Tai* [2001]
Kap Arkona	57°37′N	13°21′E	810	400	Annual	*Zier* [1991]
Leeds	53°48′N	1°34′W	1020	780–1300	Summer, Winter	*Willison et al.* [1985]
Los Angeles Basin	34°4′N	118°15′W	390	2750–4230	Annual	*Kim et al.* [2000]
Moscow	55°45′N	37°35′E	1260	3500–6750	Summer, Winter	*Kopeykin et al.* [1993]
Mount Gibbes	35°78′N	82°29′E	240	74	Winter	*Im et al.* [2001]
			200	230	Summer	
Nagoya	35°10′N	136°50′E	800	13,000	Annual	*Kadowaki* [1990]
Orleans	47°54′N	15°2′E	1180	2900	March	*Del Delumyea and Kalivretenos* [1987]
Paris	48°50′N	2°20′E	1340	4600	Annual	*Ruellan and Cachier* [2001]
			1600	13,600	Summer–Autumn	
Potsdam	52°3′N	13°4′E	1950	1000	Annual	*Zier* [1991]
Po Valley, Italy	44°39′N	11°37′E	800	1000 (500–1500)	September	*Zappoli et al.* [1999]
Radebeul	51°6′N	13°55′E	2200	1400	Annual	*Zier* [1991]
Santiago	33°33′S	70°36′W	90	30,600	June	*Didyk et al.* [2000]
Seoul	37°20′N	126°35′E	2340	8400	June	*Park et al.* [2001]
Thessaloniki	40°31′N	22°58′E	1080	3500–8900	June	*Chazette and Liousse* [2001]
Uji	34°32′N	135°29′E	860	5210	Winter	*Hitzenberger and Tohno* [2001]
			680	2600	Summer	
			770	4890	Annual	
Vienna	48°12′N	16°22′E	1370	6580	Winter	*Hitzenberger and Tohno* [2001]
			1890	2600	Summer	
			1550	4890	Annual	

Figure A.2: *Observed and modeled BC concentrations, continued.*

Table 2. Comparison of Modeled and Measured BC in Snow, Sea-Ice, and Precipitation

Site	Reference	Measurement Period	Measured BC[a], ng g^{-1}	1998 Model BC central (low-high)	2001 Model BC central (low-high)
Summit, Greenland (72.6°N, 38.5°W)	*Slater et al.* [2002]	1994–1996	14.6 (4.2–30.1)	5.2 (1.7–64.1)	3.5 (1.5–34.5)
	Cachier [1997]	1991–1995	2.0–19.0[b]		
	Chylek et al. [1995]	1989–1990	2.0 (1.5–2.7)		
	Cachier and Pertuisol [1994]	1988–1989	1.0–4.0[b]		
Camp Century, Gr. (77.2°N, 61.1°W)	*Chylek et al.* [1987]	~1985	2.4 (2.1–2.6)	13.3 (1.2–26.9)	6.2 (0.9–19.6)
Dye 3, Greenland (65.2°N, 43.8°W)	*Clarke and Noone* [1985]	May 1983	6.4 (4.3–8.5)	11.8 (3.6–131)	8.2 (3.0–29.1)
Alert, N. Canada 83.5°N, 62.5°W)	*Clarke and Noone* [1985]	Nov.-Dec. 1983	56.9 (0–127)	2.2 (0.9–5.9)	2.5 (1.0–6.0)
Greenland Sea (79.8°N, 4.2°W)	*Clarke and Noone* [1985]	Jul. 1983	38.7 (5.4–75.5)	23.9 (3.0–104)	20.4 (3.5–93.9)
Spitzbergen (79°N, 12°E)	*Clarke and Noone* [1985]	May 1983	30.9 (6.7–52)	12.7 (3.7–37.0)	7.2 (4.6–34.4)
Barrow (71.3°N, 156.6°W)	*Clarke and Noone* [1985]	Apr. 1983, Mar. 1984	22.9 (7.3–60.4)	9.7 (4.1–26.4)	8.4 (3.2–25.4)
Abisko (68.3°N, 18.5°E)	*Clarke and Noone* [1985]	Mar.-Apr. 1984	33.0 (8.8–77)	80.7 (15.3–332)	96.4 (19.4–279)
Hurricane Hill (48.0°N, 123.5°W)	*Clarke and Noone* [1985]	Mar. 1984	14.7 (10.1–18.5)	29.5 (7.1–101)	35.2 (7.1–125)
Arctic Ocean (76°N, 165°E)	*Grenfell et al.* [2002]	Mar.-Apr. 1998	4.4 (1–9)	8.4 (4.2–21.8)	5.8 (2.4–16.7)
Cascades, Wash (~47°N, 121°W)	*Grenfell et al.* [1981]	Mar. 1980	22–59	36.8 (6.3–86.3)	35.1 (6.7–85.9)
Halifax, Nova Scotia (45°N, 64°W)	*Chylek et al.* [1999]	Nov. 1995–Mar. 1996	11 (4.3–32)	84.0 (22.0–244)	84.9 (18.9–270)
French Alps (45.4°N, 5.3°E)	*Sergent et al.* [1993]	winters 1989–1991	161 (80–280)	165 (50.5–226)	136 (37.7–287)
	Sergent et al. [1998]	winters ~1992–1997	123 (34–247)		
	Fily et al. [1997]	Apr. 1992	482 (235–826)	394 (92.2–)[c]	69.4 (32.7–498)[c]
	Fily et al. [1997]	Dec. 1992	115 (22–302)	29.0 (37.4–349)	43.5 (17.6–51.5)

Figure A.3: *A selection of observed and modeled BC concentrations in snow from Flanner et al. (2007)*

Station	Modeled near-surface concentration of BC [ng/m^3]	
	Original parameterization	*M7*
Marine:		
Amsterdam Island	2.5	1.8
La Réunion Island	7	3
Mace Head, Ireland	85	200
Oki Island	20	13
San Nicolas Island	211	72
Rural:		
Abastumani	244	141
Abisko	35	28
Ecuador	174	73
Florida	142	46
K-Pustza, Hungary	685	438
North Carolina	400	247
South West U.S.	172	124
Urban:		
Beijing	730	453
Gorlitz	505	319
Halle	480	293
Hamburg	525	370
Kap Arkona	274	200
Los Angeles Basin	211	170
Nagoya	861	520
Paris	1275	1071
Potsdam	505	187
Radebeul	1073	319
Uji	861	520
Vienna	1472	1102

Figure A.4: *Near-surface concentrations modeled by the CTM2 model in this thesis for the same locations as those highlighted in figure A.1 and A.2.*

Site	Period	Modeled BC concentration in snow and ice [ng /g]	
		Original parameterization	*M7*
Dye 3, Greenland	May	1.08	0.3
Spitzbergen	May	6.7	1.7
Barrow	March	2	0.9
	April	1.08	1.06
Hurricane Hill	March	15.2	10.9
Arctic Ocean	March	3.3	1.22
	April	3	1.5
Cascades, Wash.	March	4	3.5
Halifax, Nova Scotia	March	70	10
French Alps	April	96	53

Figure A.5: *Concentrations of BC in snow modeled by the CTM2 model in this thesis at the highlighted locations in figure A.3.*

Bibliography

Ackerman, A.S.; Toon, O.B.; Stevens, D.E. and Heymsfield, A.J. (2000) *R*eduction of tropical cloudiness by soot. Science, Vol. 288.

Berge, E. (1993) *C*oupling of wet scavenging of sulphur to clouds in a numerical weather prediction model. Tellus.

Berglen, T.F.; Berntsen, T.K.; Isaksen, I.S.A. and Sundet, J.K. (2004) *A* global model of the coupled sulfur/oxidant chemistry in the troposphere: The sulfur cycle. Journal of Geophysical Research-atmospheres, Vol. 109.

Berntsen, T.K.; Fuglestvedt, J.S.; Myhre, G.; Stordal, F. and Berglen, T.F. (2006) *A*batement of greenhouse gases: Does location matter?. Climate Change.

Bond, T. (2007) *C*an warming particles enter global climate discussions. Environmental Research Letters.

Bond, T.; Dentener, F.; Kinne, S.; Boucher, O.; Cofala, J.; Generoso, S.; Ginoux, P.; Gong, S.; Hoelzemann, J.J.; Ito, A.; Marelli, L.; Penner, J.E.; Putaud, J.P.; Textor, C.; Schulz, M.; van der Werf, G.R. and Wilson, J. (2006) *E*missions of primary aerosol and precursor gases in the years 2000 and 1750 prescribed data-sets for AeroCom. Atmos. Chem. Phys., Vol. 6.

Bond, T.; Streets, D.; Fernandes, S.; Nelson, S.; Yarber, K.; Woo, J. and Klimont, Z. () *B*lack carbon inventories, Air pollution as a climate workshop. http://www.giss.nasa.gov/meetings/pollution2002/d2_bond.html.

Bond, T. and Sun, H. (2005) *C*an reducing black carbon emissions counteract global warming?. Environ. Sci. Technol., Vol. 39.

Brasseur, G.P.; Orlando, J.J. and Tyndall, G.S. (1999) *A*tmospheric Chemistry and Global Change, chapter 1 (Oxford University Press, Inc.).

Clarke, A.D. and Noone, K.J. (1985) *S*oot in the Arctic snowpack: A cause for perturbations in the radiative transfer. Atmos. Environ., Vol. 19.

Cooke, W.F.; Liousse, C. and Cachier, H. (1999) *C*onstruction of a $1^\circ x 1^\circ$ fossil fuel emission data set for carbonaceous aerosol and implementation and radiative impact in the ECHAM4 model. J. Geophys. Res., Vol. 104.

Croft, B.; Lohmann, U. and von Salzen, K. (2005) *B*lack carbon ageing in the Canadian Centre for Climate modelling and analysis of atmospheric general circulation model. Atmos. Chem. Phys., Vol. 5.

Flanner, M.G.; Zender, C.S.; Randerson, J.T. and Rasch, P.J. (2007) *P*resent-day climate forcing and response from black carbon in snow. J. Geophys. Res., Vol. 112.

Forster, P.; Ramaswamy, V.; Artaxo, P.; Berntsen, T.K.; Betts, R.; Fahey, D.W.; Haywood, J.; Lean, J.; Lowe, D.C.; Myhre, G.; Nganga, J.; Prinn, R.; Raga, G.; Schulz, M. and van Dorland, R. (2007) *C*hanges in Atmospheric Constituents and in Radiative Forcing. Climate Change 2007: The Physical Science Basis. Contribution of Working Group 1 to the Fourth Assessment Report of the Intergovernmental Panel on Climate Change.

Grenfell, T.C. and Light, B. (2002) *S*patial distribution and radiative effects of soot in the snow and sea ice during the SHEBA experiment. J. Geophys. Res., Vol. 107.

Grini, A. (2007) *I*ncluding the M7 aerosol dynamics model in the global Chemical Transport Model Oslo CTM2. Technical report, University of Oslo.

Hansen, J. and Nazarenko, L. (2004) *S*oot climate forcing via snow and ice albedos. PNAS, Vol. 101.

Hansen, J.; Sato, M.; Ruedy, R.; Lacis, A. and Oinas, V. (2000) *G*lobal warming in the twenty-first century: An alternative scenario. Proc. Natl. Acad. Sci. USA, Vol. 97.

Hansen, J.; Sato, M.; Ruedy, R.; Nazarenko, L.; Lacis, A.; Schmidt, G.A.; Russel, G.; Aleinov, I.; Bauer, M.; Bauer, S.; Bell, N.; Cairns, B.; Canuto, V.; Chandler, M.; Cheng, Y.; Genio, A. Del; Faluvegi, G.; Fleming, E.; Friend, A.; Hall, T.; Jackman, C.; Kelley, M.; Kiang, N.; Koch, D.; Lean, J.; Lerner, J.; Lo, K.; Menon, S.; Miller, R.; Minnis, P.; Novakov, T.; Oinas,

V.; Perlwitz, Ja.; Perlwitz, Ju.; Rind, D.; Romanou, A.; Shindell, D.; Stone, P.; Sun, S.; Tausnev, N.; Thresher, D.; Wielicki, B.; Wong, T.; Yao, M. and Zhang, S. (2005) *E*fficacy of climate forcings. J. Geophys. Res., Vol. 110.

http://sealevel.jpl.nasa.gov/overview/climate-climatic.html () .

http://www.cgrer.uiowa.edu/EMISSION_DATA_new/summary_of_changes.html () .

IPCC, 2007 () *C*limate Change 2007: Synthesis Report. Contribution of Working Groups I, II and III to the Fourth Assessment Report of the Intergovernmental Panel on Climate Change [Core Writing Team, Pachuri, R.K. and Reisinger, A. (eds.)]. IPCC, Geneva, Switzerland, 104 pp..

Jacobs, D.J. (1999) *I*ntroduction to atmosheric chemistry, chapter 3 (Princeton University Press).

Jacobson, M.Z. (2002) *C*ontrol of fossil fuel black carbon and organic matter, possibly the most effective method of slowing global warming. J. Geophys. Res., Vol. 107.

Jacobson, M.Z. (2004) *C*limate response of fossil fuel soot, accounting for soot's feedback to snow and sea ice albedo and emissivity. J. Geophys. Res., Vol. 109.

Johnson, B.T.; Shine, K.P. and Forster, P.M. (2004) *T*he semi-direct effect: Impact of absorbing aerosols on marine stratocumulus. Q.J.R. Meteorol. Soc., Vol. 130.

Klonecki, A.; Hess, P.; Emmons, L.; Smith, L. and Orlando, J. (2003) *S*easonal changes in the transport of pollutants into the Arctic troposphere-model study. J. Geophys. Res., Vol. 108.

Koch, D.; Bond, T.; Streets, D.; Unger, N. and van der Werf, G. R. (2007) *G*lobal impacts from aerosols from particular source regions and sectors. J. Geophys. Res., Vol. 112.

Koch, D. and Hansen, J. (2005) *D*istant origins of Arctic black carbon: A Goddard Institute for Space Studies Model Experiment. J. Geophys. Res., Vol. 110.

Koren, I.; Kaufman, Y.J.; Remer, L.A. and Martins, J.V. (2004) *M*easurements of the effect of Amazon smoke on inhibition of cloud formation. Science, Vol. 303.

Kvissel, O.K. (2007) *V*alidating Oslo CTM2 using MIPAS IMK-IAA satellite data from 2003. Master thesis, University of Oslo.

Law, K.S. and Stohl, A. (2007) *A*rctic air pollution: Origins and Impacts. Science, Vol. 315.

Lemke, P.; Ren, J.; Alley, R.B.; Allison, I.; Carrasco, J.; Flato, G.; Fujii, Y.; Kaser, G.; Mote, P.; Thomas, R.H. and Zhang, T. (2007) *O*bservations: Changes in Snow, Ice and Frozen Ground. Climate Change 2007: The Physical Science Basis. Contribution of Working Group I to the Fourth Assessment Report of the Intergovernmental Panel on Climate change.

Lohmann, U. and Diehl, K. (2005) *S*ensitivity studies of the importance of dust ice nuclei for the indirect aerosol effect on stratiform mixed-phase clouds. Journal of Atmospheric Sciences, Vol. 63.

Lohmann, U. and Feichter, J. (2005) *G*lobal indirect aerosol effect: a review. Atm. Chem. Phys., Vol. 5.

Magono, C.; Endoh, T.; nd S. Kubota, F. Ueno and Itasaka, M. (1979) *D*irect observations of aerosols attached to falling snow crystals. Tellus, Vol. 31.

Maria, S.F.; Russell, L.M.; Gilles, M.K. and Myeni, S.C.B. (2004) *O*rganic Aerosol Growth Mechanisms and Their Climate-Forcing Implications. Science, Vol. 306.

McConnel, J.R.; Edwards, R.; Kok, G.L.; Flanner, M.G.; Zender, C.S.; Saltzman, E.S.; Banta, J.R.; Pasteris, D.R.; Carter, M.M. and Kahl, J.D.W. (2007) *2*0th-Century Industrial Black Carbon Emissions Altered Arctic Climate Forcing. Science, Vol. 317.

Myhre, G.; Berglen, T.F.; Johnsrud, M.; Hoyle, C.; Berntsen, T.K.; Christopher, S.A.; Isaksen, I.S.A.; Jones, T.A.; Kahn, R.A.; Loeb, N.; Quinn, P.; Remer, L. and Yttri, K.E. (2008) *R*adiative forcing of the direct aerosol effect using a multi-observation approach. Submittet ACP.

Novakov, T.; Ramanathan, V.; Hansen, J.E.; Kirchstetter, T.W.; Sato, M.; Sinton, J.E. and Sathye, J.A. (2003) *L*arge historical changes of fossil-fuel black carbon aerosols. Geophys. Res. Lett., Vol. 30.

Prather, M.J. (1986) *N*umerical advection by conservation of second-order moments. J. Geophys. Res., Vol. 91.

Quinn, P.K.; Shaw, G.; Andrews, E.; Dutton, E.G.; Ruoho-airola, T. and S.L.Gong (2007) *A*rctic Haze: current trends and knowledge gaps. Tellus B, Vol. 59.

Ramanathan, V. and Carmichael, G. (2008) *G*lobal and regional climate changes due to black carbon. Nature geoscience.

Randerson, J.T.; van der Werf, G.R.; Giglio, L.; Collatz, G.J. and Kasibhatla, P.S. (2007) *G*lobal Fire Emission Database, version 2.1 (GFEDv2.1) data set. Available on-line (http://daac.ornl.gov) from Oak Ridge National Laboratory Distributed Active Archive Center, Oak Tidge, Tennessee, U.S.A.

Reddy, M. S. and Boucher, O. (2007) *C*limate impact of black carbon emitted from energy consumption in the world's regions. Geophys. Res. Lett., Vol. 34.

Rypdal, K.; Berntsen, T.; Fuglestvedt, J.S.; Aunan, K.; Torvanger, A.; Stordal, F.; Pacyna, J.M. and Nygaard, L.P. (2005) *T*ropospheric ozone and aerosols in climate agreements: scientific and political challenges. Environmental science and policy.

Schulz, M.; Textor, C.; Kinne, S.; Balkanski, Y.; Bauer, S.; Berntsen, T.K.; Berglen, T.F.; Boucher, O.; Dentener, F.; Guibert, S.; Isaksen, I.S.A.; Iversen, T.; Koch, D.; Kirkevåg, A.; Liu, X.; Montanaro, V.; Myhre, G.; Penner, J.E.; Pitari, G.; Reddy, S.; Seland, Ø.; Stier, P. and Takemura, T. (2006) *R*adiative forcing by aerosols as derived from the present-day and pre-industrial simulations. Atmos. Chem. Phys., Vol. 6: p. 5225–5246.

Sharma, S.; Andrews, E.; Barrie, L.A.; Ogren, J.A. and Lavoue, D. (2006) *V*ariations and sources of equivalent black carbon in high Arctic revealed by long-term observations at Alert and Barrow: 1989-2003. J. Geophys. Res., Vol. 111.

Shindell, D.T.; Teich, H.; Chin, M.; Dentener, F.; Doherty, R.M.; Faluvegi, G.; Fiore, A.M.; Hess, P.; MacKenzie, I.A.; Sanderson, M.G.; Schultz, M.G.; Schulz, M.; Stevenson, D.S.; Textor, C.; Wild, O.; Bergmann, D.J.; ans C. Cuvelier, H. Bian; Duncan, B.N.; Folberth, G.; Horowitz, L.W.; Jonson, J.; Kaminski, J.W.; Marmer, E.; Park, R.; Pringle, K.J.; Schroeder, S.; Szopa, S.; Takemura, T.; Zeng, G.; Keating, T.J. and Zuber, A. (2008) *A* multi-model assessment of pollution transport to the Arctic. Atmos. Chem. Phys. Discuss., Vol. 8.

Skeie, R.B. (2007) *M*odel description. Snow/ice deposition routine.

Slater, J.F.; Currie, L.A.; Dibb, J.E. and Jr., B.A. Benner (2002) *D*istinguishing the relative contribution of fossil fuel and biomass burning combustion aerosols deposited at Summit, Greenland through isotopic and molecular characterization of insoluble carbon. Atmospheric Environment.

Stohl, A. (2006) *C*haracteristics of atmospheric transport into the Arctic troposphere. J. Geophys. Res., Vol. 111.

Tiedtke, M. (1989) *A* comprehensive mass flux scheme for cumulus parameterization in large-scale models. Monthly Weather Review, Vol. 117.

UNEP, 2007 () *G*lobal outlook for ice and snow, United Nations Environment Programme. An official project of the International Polar Year 2007-2008.

Vestreng, V.; Myhre, G.; Fagerli, H.; Reis, S. and Tarrason, L. (2007) *T*wenty-five years of continuous sulphur dioxide emissionreduction in Europe. Atm. Chem. Phys., Vol. 7.

Vignati, E. and Wilson, J. (2004) *M7*: An efficient size-resolved aerosol microphysics module for large-scale aerosol transport models. J. Geophys. Res., Vol. 109.

Warren, S.; Grenfell, T. and Clarke, A. (2005) *P*roject summary. Black carbon in snow and ice, and its effects on surface albedo.

Warren, S.G. and Wiscombe, W.J. (1980) *A* model for the spectral albedo of snow. II:Snow containing atmospheric aerosols. Journal of Atmospheric Sciences.

WWF Nepal Program, March 2005 () *A*n overview of glaciers, glacier retreat, and subsequent impacts in Nepal, India and China.